



HAL
open science

Convergence of a Vertex centred Discretization of Two-Phase Darcy flows on General Meshes

Konstantin Brenner, Roland Masson

► **To cite this version:**

Konstantin Brenner, Roland Masson. Convergence of a Vertex centred Discretization of Two-Phase Darcy flows on General Meshes. *International Journal on Finite Volumes*, 2013, 10, pp.1-37. hal-00755072v2

HAL Id: hal-00755072

<https://hal.science/hal-00755072v2>

Submitted on 27 Nov 2013

HAL is a multi-disciplinary open access archive for the deposit and dissemination of scientific research documents, whether they are published or not. The documents may come from teaching and research institutions in France or abroad, or from public or private research centers.

L'archive ouverte pluridisciplinaire **HAL**, est destinée au dépôt et à la diffusion de documents scientifiques de niveau recherche, publiés ou non, émanant des établissements d'enseignement et de recherche français ou étrangers, des laboratoires publics ou privés.

Convergence of a Vertex centered Discretization of Two-Phase Darcy flows on General Meshes

K. Brenner

*University of Nice Sophia Antipolis, and team COFFEE, INRIA Sophia Antipolis
Méditerranée, France*

Tel.: +33 4 92 07 69 96

konstantin.brenner@unice.fr

R. Masson

*University of Nice Sophia Antipolis, and team COFFEE, INRIA Sophia Antipolis
Méditerranée, France*

Tel.: +33 4 92 07 62 32

roland.masson@unice.fr

Abstract

This article analyses the convergence of the Vertex Approximate Gradient (VAG) scheme recently introduced in Eymard et al. 2012 for the discretization of multiphase Darcy flows on general polyhedral meshes. The convergence of the scheme to a weak solution is shown in the particular case of an incompressible immiscible two-phase Darcy flow model with capillary diffusion using a global pressure formulation. A remarkable property in practice is that the convergence is proven whatever the distribution of the volumes at the cell centers and at the vertices used in the control volume discretization of the saturation equation. The numerical experiments carried out for various families of 2D and 3D meshes confirm this result on a one-dimensional Buckley Leverett solution.

Key words : Finite volume, two-phase Darcy flows, diffusion fluxes, general meshes, heterogeneous anisotropic media

1 Introduction

Recently, a new discretization of diffusive equations, the Vertex Approximate Gradient (VAG) scheme, using both cell and vertex unknowns, has been introduced in [16]. The cell unknowns can be eliminated locally without any fill-in in the

sense that no additional connections between vertices are introduced in the elimination. It leads after elimination of the cell unknowns to a vertex-centered scheme with a typical 27 points stencil for 3D topologically Cartesian meshes. The VAG scheme is consistent, unconditionally coercive, compact, and easy to implement on general polyhedral meshes (with possibly non planar faces) and for heterogeneous anisotropic diffusion tensors. In addition, it is exact on cellwise affine solutions for cellwise constant diffusion tensors. It has exhibited a good compromise between accuracy, robustness and CPU time in the recent FVCA6 3D benchmark [15].

The VAG scheme has been extended to multiphase Darcy flows in [18] and [17] and leads to a conservative finite volume discretization with fluxes connecting each cell to its vertices. It can be viewed as a control volume method widely used in the oil industry (see [3] and [21]) provided that control volumes are defined both at the cell centers and at the vertices.

Compared with usual cell-centered finite volume approaches, the main interests of the VAG discretization are twofold: first the single phase Darcy fluxes lead to a coercive discretization for arbitrary cells and permeability tensors and second the cell unknowns can still be eliminated without fill-in from the linear system leading to a large reduction of the set of unknowns in the case of tetrahedral meshes compared with cell-centered approaches.

Compared with control volume finite element discretizations introduced in [4] and which have been applied to multiphase Darcy flows for example in [19], [7], the VAG fluxes are not defined as the integral of the normal velocity on a dual mesh interfaces. This allows us to decouple the definition of the fluxes from the definition of the control volumes. This is why we can obtain coercive single phase Darcy fluxes for arbitrary cells and permeability tensors which is not the case for control volume finite element methods. In addition, in our method, we only need to define a volume at each vertex and at each cell which are simply obtained by any conservative redistribution of the volume of each cell to its vertices preserving the non negativity of the remaining volumes at the cells. In practice these volumes are distributed in order first to respect the main heterogeneities of the porous media and second to balance as much as possible the volumes between the surrounding cells and vertices (see [17]).

The main objective of this paper is to strenghten the theoretical background of this approach by proving the convergence of the VAG discretization whatever the choice of the volumes at the cell centers and at the vertices in the particular case of a two-phase incompressible immiscible Darcy flow model.

The first convergence result for a finite volume discretization of two-phase Darcy flow models has been obtained for cell-centered two point flux approximation schemes on admissible meshes in [20] and [12]. In [12] the convergence is obtained for the usual phase pressures and saturations formulation using a phase by phase upwinding of the mobilities. To our knowledge, this is the only convergence result for such a formulation widely used in petroleum engineering and the proof uses crucially the two point nature of the flux approximation. In [20] the convergence is obtained for the global pressure formulation introduced in [6] (see also [2]). This latter convergence result has been recently extended in [5] to the case of the Sushi finite volume

discretization [13] which applies to general polyhedral meshes and heterogeneous anisotropic porous media. Let us also quote [8] providing error estimates for the two phase Darcy flow model in global pressure formulation using a Mixed Finite Element Method for the pressure equation and a Finite Element discretization of the saturation equation.

Our proof is an adaptation of the result given in [5] for the Sushi scheme in global pressure formulation to the case of the VAG discretization. One of the main additional difficulty is to show the convergence of the scheme whatever the choice of the volumes at the cell centers and at the vertices. This requires to work with different representations of the discrete saturation for which we need to estimate their differences in L^2 norm, as well as to derive new discrete Poincaré inequalities.

The outline of the paper is the following. We first recall in section 2 the VAG discretization for a diffusion equation on general polyhedral meshes and derive the VAG fluxes between each cell and its vertices. In section 3, the two-phase flow model and its VAG discretization are introduced. They rely on the so-called global pressure formulation and on a fully implicit Euler integration in time. The VAG discretization is used for the Darcy fluxes as well as for the capillary diffusion, and the fractional flow term is approximated using a first order upwind scheme. Then, the weak convergence of the discrete pressure and the strong convergence of the discrete saturation to a weak solution of the two-phase flow problem are derived up to a subsequence. In section 4, the convergence of the scheme is assessed on a Buckley Leverett one-dimensional solution for various families of 2D and 3D meshes mainly taken from the FVCA5 and FVCA6 [15] benchmarks.

2 Vertex centered Discretization on generalised polyhedral meshes

2.1 Vertex Approximate Gradient discretization of the Darcy fluxes

Let Ω be a bounded polyhedral subdomain of \mathbb{R}^3 of boundary $\partial\Omega = \bar{\Omega} \setminus \Omega$.

For a.e. (almost every) $\mathbf{x} \in \Omega$, $\Lambda(\mathbf{x})$ denotes a 3-dimensional symmetric positive definite matrix such that there exist $\bar{\Lambda} \geq \underline{\Lambda} > 0$ with

$$\underline{\Lambda}\|\xi\|^2 \leq \xi^t \Lambda(\mathbf{x}) \xi \leq \bar{\Lambda}\|\xi\|^2,$$

for all $\xi \in \mathbb{R}^3$ and for a.e. $\mathbf{x} \in \Omega$.

We consider the following diffusion equation

$$\begin{cases} \operatorname{div}(-\Lambda \nabla \bar{u}) = f & \text{in } \Omega, \\ \bar{u} = 0 & \text{on } \partial\Omega, \end{cases}$$

with homogeneous Dirichlet boundary condition. Its variational formulation: find $\bar{u} \in H_0^1(\Omega)$ such that

$$\int_{\Omega} \Lambda \nabla \bar{u} \cdot \nabla v \, d\mathbf{x} = \int_{\Omega} f v \, d\mathbf{x}$$

for all $v \in H_0^1(\Omega)$, admits a unique solution \bar{u} provided that $f \in L^2(\Omega)$ which is assumed in the following.

Following [16], we consider generalised polyhedral meshes of Ω . Let \mathcal{M} be the set of cells that are disjoint open subsets of Ω such that $\bigcup_{\kappa \in \mathcal{M}} \bar{\kappa} = \bar{\Omega}$. For all $\kappa \in \mathcal{M}$, \mathbf{x}_κ denotes the so-called ‘‘center’’ of the cell κ under the assumption that κ is star-shaped with respect to \mathbf{x}_κ . Let \mathcal{F} denote the set of faces of the mesh which are not assumed to be planar, hence the term ‘‘generalised polyhedral cells’’. We denote by \mathcal{V} the set of vertices of the mesh. Let \mathcal{V}_κ , \mathcal{F}_κ , \mathcal{V}_σ respectively denote the set of the vertices of $\kappa \in \mathcal{M}$, faces of κ , and vertices of $\sigma \in \mathcal{F}$. For any face $\sigma \in \mathcal{F}_\kappa$, we have $\mathcal{V}_\sigma \subset \mathcal{V}_\kappa$. Let $\mathcal{M}_\mathbf{s}$ denote the set of the cells sharing the vertex \mathbf{s} . The set of edges of the mesh is denoted by \mathcal{E} and \mathcal{E}_σ denotes the set of edges of the face $\sigma \in \mathcal{F}$. It is assumed that for each face $\sigma \in \mathcal{F}$, there exists a so-called ‘‘center’’ of the face \mathbf{x}_σ such that

$$\mathbf{x}_\sigma = \sum_{\mathbf{s} \in \mathcal{V}_\sigma} \beta_{\sigma,\mathbf{s}} \mathbf{x}_\mathbf{s}, \quad \text{with} \quad \sum_{\mathbf{s} \in \mathcal{V}_\sigma} \beta_{\sigma,\mathbf{s}} = 1,$$

where $\beta_{\sigma,\mathbf{s}} \geq 0$ for all $\mathbf{s} \in \mathcal{V}_\sigma$. The face σ is assumed to match with the union of the triangles $T_{\sigma,e}$ defined by the face center \mathbf{x}_σ and each of its edge $e \in \mathcal{E}_\sigma$.

Let $\mathcal{V}_{int} = \mathcal{V} \setminus \partial\Omega$ denote the set of interior vertices, and $\mathcal{V}_{ext} = \mathcal{V} \cap \partial\Omega$ the set of boundary vertices.

The previous discretization is denoted by \mathcal{D} and we define the discrete space

$$W_{\mathcal{D}} = \{v_\kappa \in \mathbb{R}, v_\mathbf{s} \in \mathbb{R}, \kappa \in \mathcal{M}, \mathbf{s} \in \mathcal{V}\},$$

and its subspace with homogeneous Dirichlet boundary conditions on \mathcal{V}_{ext}

$$W_{\mathcal{D}}^0 = \{v_\kappa \in \mathbb{R}, v_\mathbf{s} \in \mathbb{R}, \kappa \in \mathcal{M}, \mathbf{s} \in \mathcal{V} \mid v_\mathbf{s} = 0 \text{ for } \mathbf{s} \in \mathcal{V}_{ext}\}.$$

The VAG scheme introduced in [16] is based on a piecewise constant discrete gradient reconstruction for functions in the space $W_{\mathcal{D}}$. Several constructions are proposed based on different decompositions of the cell. Let us recall the simplest one based on a conforming finite element discretization on a tetrahedral sub-mesh, and we refer to [16, 14] for two other constructions sharing the same basic features.

For all $\sigma \in \mathcal{F}$, the operator $I_\sigma : W_{\mathcal{D}} \rightarrow \mathbb{R}$ such that

$$I_\sigma(v) = \sum_{\mathbf{s} \in \mathcal{V}_\sigma} \beta_{\sigma,\mathbf{s}} v_\mathbf{s},$$

is by definition of \mathbf{x}_σ a second order interpolation operator at point \mathbf{x}_σ .

Let us introduce the tetrahedral sub-mesh $\mathcal{T} = \{T_{\kappa,\sigma,e}, e \in \mathcal{E}_\sigma, \sigma \in \mathcal{F}_\kappa, \kappa \in \mathcal{M}\}$ of the mesh \mathcal{M} , where $T_{\kappa,\sigma,e}$ is the tetrahedron defined by the cell center \mathbf{x}_κ and the triangle $T_{\sigma,e}$ as shown by Figure 1.

For a given $v \in W_{\mathcal{D}}$, we define the function $\pi_{\mathcal{T}}v \in H^1(\Omega)$ as the continuous piecewise affine function on each tetrahedron T of \mathcal{T} such that $\pi_{\mathcal{T}}v(\mathbf{x}_{\kappa}) = v_{\kappa}$, $\pi_{\mathcal{T}}v(\mathbf{s}) = v_{\mathbf{s}}$, and $\pi_{\mathcal{T}}v(\mathbf{x}_{\sigma}) = I_{\sigma}(v)$ for all $\kappa \in \mathcal{M}$, $\mathbf{s} \in \mathcal{V}$, $\sigma \in \mathcal{F}$. We define the space $V_{\mathcal{T}} = \{\pi_{\mathcal{T}}v, v \in W_{\mathcal{D}}\} \subset H^1(\Omega)$ and the space $V_{\mathcal{T}}^0 = \{\pi_{\mathcal{T}}v, v \in W_{\mathcal{D}}^0\}$, which lies in $H_0^1(\Omega)$. The nodal basis of this finite element discretization will be denoted by $\eta_{\kappa}, \eta_{\mathbf{s}}, \kappa \in \mathcal{M}, \mathbf{s} \in \mathcal{V}$.

Following [16], the Vertex Approximate Gradient (VAG) scheme is defined by the discrete variational formulation: find $u \in W_{\mathcal{D}}^0$ such that

$$a_{\mathcal{D}}(u, v) = \int_{\Omega} f(\mathbf{x}) \pi_{\mathcal{T}}v(\mathbf{x}) \, d\mathbf{x} \quad \text{for all } v \in W_{\mathcal{D}}^0,$$

with $a_{\mathcal{D}}$ the bilinear form defined by

$$a_{\mathcal{D}}(u, v) = \int_{\Omega} \nabla \pi_{\mathcal{T}}u(\mathbf{x}) \cdot \Lambda(\mathbf{x}) \nabla \pi_{\mathcal{T}}v(\mathbf{x}) \, d\mathbf{x} \quad \text{for all } (u, v) \in W_{\mathcal{D}}^0 \times W_{\mathcal{D}}^0.$$

Let us define for all $\kappa \in \mathcal{M}$ and $\mathbf{s}, \mathbf{s}' \in \mathcal{V}_{\kappa}$

$$a_{\kappa, \mathbf{s}}^{\mathbf{s}'} = \int_{\kappa} \nabla \eta_{\mathbf{s}}(\mathbf{x}) \cdot \Lambda(\mathbf{x}) \nabla \eta_{\mathbf{s}'}(\mathbf{x}) \, d\mathbf{x}.$$

One has

$$a_{\mathcal{D}}(u, v) = \sum_{\kappa \in \mathcal{M}} \sum_{\mathbf{s} \in \mathcal{V}_{\kappa}} \sum_{\mathbf{s}' \in \mathcal{V}_{\kappa}} a_{\kappa, \mathbf{s}}^{\mathbf{s}'} (u_{\mathbf{s}'} - u_{\kappa})(v_{\mathbf{s}} - v_{\kappa}),$$

leading to the definition of the following conservative fluxes between a given cell $\kappa \in \mathcal{M}$ and its vertices $\mathbf{s} \in \mathcal{V}_{\kappa}$

$$F_{\kappa, \mathbf{s}}(u) = \sum_{\mathbf{s}' \in \mathcal{V}_{\kappa}} a_{\kappa, \mathbf{s}}^{\mathbf{s}'} (u_{\kappa} - u_{\mathbf{s}'}) = - \int_{\kappa} \Lambda(\mathbf{x}) \nabla \pi_{\mathcal{T}}u \cdot \nabla \eta_{\mathbf{s}} \, d\mathbf{x}, \quad (1)$$

and

$$F_{\mathbf{s}, \kappa}(u) = -F_{\kappa, \mathbf{s}}(u).$$

Then, the VAG discretization is equivalent to the following discrete system of conservation laws: find $u \in W_{\mathcal{D}}^0$ such that

$$\left\{ \begin{array}{l} \sum_{\mathbf{s} \in \mathcal{V}_{\kappa}} F_{\kappa, \mathbf{s}}(u) = \int_{\kappa} f(\mathbf{x}) \eta_{\kappa}(\mathbf{x}) \, d\mathbf{x} \quad \text{for all } \kappa \in \mathcal{M}, \\ \sum_{\kappa \in \mathcal{M}_{\mathbf{s}}} F_{\mathbf{s}, \kappa}(u) = \int_{\Omega} f(\mathbf{x}) \eta_{\mathbf{s}}(\mathbf{x}) \, d\mathbf{x} \quad \text{for all } \mathbf{s} \in \mathcal{V}_{int}. \end{array} \right.$$

3 Convergence analysis for a two-phase flow model

We consider the following two-phase incompressible Darcy flow model. The gravity is not considered for the sake of simplicity but all the subsequent convergence analysis

extends to the case with gravity following the same arguments as in [5].

$$\left\{ \begin{array}{l} \operatorname{div}(-\lambda(S) \Lambda \nabla p) = k^+ + k^- \text{ on } Q_{t_f}, \\ \phi \partial_t S + \operatorname{div}(-f(S)\lambda(S) \Lambda \nabla p) + \operatorname{div}(-\Lambda \nabla \varphi(S)) = k^o(\cdot, S) \text{ on } Q_{t_f}, \\ k^o(\cdot, S) = f(S^{\text{inj}})k^+ + f(S)k^- \text{ on } Q_{t_f}, \\ S = 0, p = 0 \text{ on } \partial\Omega \times (0, t_f), \\ S|_{t=0} = S_0 \text{ on } \Omega, \end{array} \right. \quad (2)$$

where $Q_{t_f} := \Omega \times (0, t_f)$. Let us refer to [9] for an existence of a weak solution and a uniqueness result for such a two phase Darcy flow model.

Assumptions on the data :

(\mathcal{H}_1) $\varphi \in C([0, 1])$, $\varphi(0) = 0$, is a strictly increasing piecewise continuously differentiable Lipschitz-continuous function with a Lipschitz constant L_φ .

(\mathcal{H}_2) The functions $\lambda, f \in C([0, 1])$ are Lipschitz-continuous; we denote by L_λ and L_f the corresponding Lipschitz constants.

(\mathcal{H}_3) λ is such that $0 < \underline{\lambda} \leq \lambda(s)$ for all $s \in [0, 1]$;

(\mathcal{H}_4) f is a nondecreasing function and it satisfies $f(0) = 0, f(1) = 1$;

(\mathcal{H}_5) $S_0 \in L^\infty(\Omega)$; and $\phi \in L^\infty(\Omega)$ is such that $0 < \underline{\phi} \leq \phi(\mathbf{x}) \leq \bar{\phi}$ for a.e. in $\mathbf{x} \in \Omega$;

(\mathcal{H}_6) $k^+, k^- \in L^\infty(\Omega)$ are such that $k^+ \geq 0, k^- \leq 0$ a.e. in Ω , $S^{\text{inj}} \in L^\infty(\Omega)$ is such that $S^{\text{inj}} \in [0, 1]$ a.e. in Ω .

The scheme that we propose does not guarantee that S remains in $[0, 1]$, thus we have to extend all the functions of S on \mathbb{R} , which is done in following way.

(\mathcal{H}_7) The functions λ, f are continuously extended by a constant outside of $(0, 1)$; φ is linear outside of $[0, 1]$ with $\varphi(s) = L_\varphi s$ for all $s < 0$ and $\varphi(s) - \varphi(1) = L_\varphi(s - 1)$ for all $s > 1$.

Weak solution :

A function pair (S, p) is a weak solution of the problem (2) if

- (i) $S \in L^2(0, t_f; L^2(\Omega))$;
- (ii) $\varphi(S) \in L^2(0, t_f; H_0^1(\Omega))$;
- (iii) $p \in L^\infty(0, t_f; H_0^1(\Omega))$;
- (iv) for all $\psi \in L^2(0, t_f; H_0^1(\Omega))$ with $\partial_t \psi \in L^2(Q_{t_f})$, $\psi(\cdot, T) = 0$, S and p satisfy

the integral equalities

$$\begin{aligned}
 - \int_0^{t_f} \int_{\Omega} S \partial_t \psi \, d\mathbf{x} dt - \int_{\Omega} S_0 \psi(\cdot, 0) \, d\mathbf{x} + \int_0^{t_f} \int_{\Omega} f(S) \lambda(S) \Lambda \nabla p \cdot \nabla \psi \, d\mathbf{x} dt \\
 + \int_0^{t_f} \int_{\Omega} \Lambda \nabla \varphi(S) \cdot \nabla \psi \, d\mathbf{x} dt = \int_0^{t_f} \int_{\Omega} k^o(\cdot, S) \psi \, d\mathbf{x} dt,
 \end{aligned} \tag{3}$$

and

$$\int_0^{t_f} \int_{\Omega} \lambda(S) \Lambda \nabla p \cdot \nabla \psi \, d\mathbf{x} dt = \int_0^{t_f} \int_{\Omega} (k^+ + k^-) \psi \, d\mathbf{x} dt.$$

VAG discretization of the two-phase flow model:

Let us denote by $|\kappa|$ the volume of the cell κ : $|\kappa| = \int_{\kappa} d\mathbf{x}$. Let us introduce the weights $\alpha_{\kappa}^{\mathbf{s}} \geq 0$, $\kappa \in \mathcal{M}$, $\mathbf{s} \in \mathcal{V}_{\kappa} \cap \mathcal{V}_{int}$ representing the fractions of volume of a cell κ distributed to a vertex \mathbf{s} of the cell κ . They are chosen such that the remaining volume at each cell is non negative i.e. $\left(1 - \sum_{\mathbf{s} \in \mathcal{V}_{\kappa} \cap \mathcal{V}_{int}} \alpha_{\kappa}^{\mathbf{s}}\right) \geq 0$ for all $\kappa \in \mathcal{M}$.

Then, we define the volumes

$$\left\{ \begin{array}{ll} m_{\kappa, \mathbf{s}} = \alpha_{\kappa}^{\mathbf{s}} |\kappa| & \text{for all } \kappa \in \mathcal{M}, \mathbf{s} \in \mathcal{V}_{\kappa} \cap \mathcal{V}_{int}, \\ m_{\mathbf{s}} = \sum_{\kappa \in \mathcal{M}_{\mathbf{s}}} m_{\kappa, \mathbf{s}} & \text{for all } \mathbf{s} \in \mathcal{V}_{int}, \\ m_{\kappa} = |\kappa| - \sum_{\mathbf{s} \in \mathcal{V}_{\kappa} \cap \mathcal{V}_{int}} m_{\kappa, \mathbf{s}} & \text{for all } \kappa \in \mathcal{M}, \end{array} \right. \tag{4}$$

which are such that

$$\sum_{\nu \in \mathcal{M} \cup \mathcal{V}_{int}} m_{\nu} = \sum_{\kappa \in \mathcal{M}} |\kappa| = \int_{\Omega} d\mathbf{x}.$$

Let $\omega_{\kappa}, \omega_{\kappa, \mathbf{s}}, \mathbf{s} \in \mathcal{V}_{\kappa} \cap \mathcal{V}_{int}$ be some partition of the cell κ such that $\int_{\omega_{\kappa}} d\mathbf{x} = m_{\kappa}$ and $\int_{\omega_{\kappa, \mathbf{s}}} d\mathbf{x} = m_{\kappa, \mathbf{s}}$, and let us set $\omega_{\mathbf{s}} = \bigcup_{\kappa \in \mathcal{M}_{\mathbf{s}}} \omega_{\kappa, \mathbf{s}}$ for all $\mathbf{s} \in \mathcal{V}_{int}$. Let the porosity ϕ_{ν} of each $\nu \in \mathcal{M} \cup \mathcal{V}_{int}$ be defined such that

$$m_{\nu} \phi_{\nu} = \int_{\omega_{\nu}} \phi(\mathbf{x}) \, d\mathbf{x},$$

and arbitrarily chosen in the interval $[\underline{\phi}, \bar{\phi}]$ for a vanishing volume m_{ν} . It results from the hypothesis \mathcal{H}_5 that

$$\underline{\phi} \leq \phi_{\nu} \leq \bar{\phi} \text{ for all } \nu \in \mathcal{M} \cup \mathcal{V}_{int}. \tag{5}$$

Our main objective is to prove the convergence of the VAG scheme for the above two-phase flow model whatever the choice of the volume fractions $\alpha_{\kappa}^{\mathbf{s}}$. This flexibility in the choice of the volumes is a key feature to adapt the VAG scheme for two-phase flows in heterogeneous media. In that case, as explained in [17], the volume fraction $\alpha_{\kappa}^{\mathbf{s}}$ is chosen proportional to the ratio between the permeability of the cell κ and the sum of the permeabilities of all cells around the vertex \mathbf{s} . This choice is modified in the case of different rocktypes in the cells around the vertex \mathbf{s} in such a way that only cells sharing the same given rocktype distribute a non zero fraction of their

volume to the vertex \mathbf{s} . This guarantees that the rocktype is uniquely defined at the vertex \mathbf{s} . We refer to [17] for details.

The spatial VAG discretization of the two-phase flow model (2) is obtained following [17] writing the mass conservation of both phases in the control volumes ω_κ and $\omega_{\mathbf{s}} = \bigcup_{\kappa \in \mathcal{M}_{\mathbf{s}}} \omega_{\kappa, \mathbf{s}}$ using the VAG fluxes $F_{\kappa, \mathbf{s}}$.

For the sake of simplicity, for $N \in \mathbb{N}^*$, we will consider the uniform time discretization $t^n = n \frac{t_f}{N}$, $n = 0, \dots, N$, of the time interval $[0, t_f]$ with $t^0 = 0$, $t^N = t_f$ and with the constant time step $\Delta t = \frac{t_f}{N}$. We consider an Euler implicit time discretization scheme. Thus, we obtain the following set of discrete equations:

$$\left\{ \begin{array}{l} \sum_{\mathbf{s} \in \mathcal{V}_\kappa} V_{\kappa, \mathbf{s}}^n = m_\kappa (k_\kappa^+ + k_\kappa^-), \quad \kappa \in \mathcal{M}, \quad (6) \\ \sum_{\kappa \in \mathcal{M}_{\mathbf{s}}} -V_{\kappa, \mathbf{s}}^n = m_{\mathbf{s}} (k_{\mathbf{s}}^+ + k_{\mathbf{s}}^-), \quad \mathbf{s} \in \mathcal{V}_{int}, \quad (7) \\ \phi_\kappa m_\kappa \frac{S_\kappa^n - S_\kappa^{n-1}}{\Delta t} + \sum_{\mathbf{s} \in \mathcal{V}_\kappa} f(S_{\kappa, \mathbf{s}}^n) V_{\kappa, \mathbf{s}}^n + F_{\kappa, \mathbf{s}}(\varphi(S^n)) = m_\kappa k_\kappa^{o, n}, \quad \kappa \in \mathcal{M}, \quad (8) \\ \phi_{\mathbf{s}} m_{\mathbf{s}} \frac{S_{\mathbf{s}}^n - S_{\mathbf{s}}^{n-1}}{\Delta t} + \sum_{\kappa \in \mathcal{M}_{\mathbf{s}}} -f(S_{\kappa, \mathbf{s}}^n) V_{\kappa, \mathbf{s}}^n - F_{\kappa, \mathbf{s}}(\varphi(S^n)) = m_{\mathbf{s}} k_{\mathbf{s}}^{o, n}, \quad \mathbf{s} \in \mathcal{V}_{int}, \quad (9) \\ V_{\kappa, \mathbf{s}}^n = \lambda(S_\kappa^n) F_{\kappa, \mathbf{s}}(p^n), \quad \mathbf{s} \in \mathcal{V}_\kappa, \kappa \in \mathcal{M}, \\ k_\nu^{o, n} = k_\nu^+ f(S_\nu^{inj}) + k_\nu^- f(S_\nu^n), \quad \nu \in \mathcal{M} \cup \mathcal{V}_{int}, \\ S_{\mathbf{s}}^n = 0, p_{\mathbf{s}}^n = 0, \quad \mathbf{s} \in \mathcal{V}_{ext}, \quad (10) \end{array} \right.$$

for all $n = 1, \dots, N$, where for all functions $\beta = S^0, S^{inj}, k^+, k^-, \beta_\nu$ is defined for all $\nu \in \mathcal{M} \cup \mathcal{V}_{int}$ by

$$m_\nu \beta_\nu = \int_{\omega_\nu} \beta(\mathbf{x}) \, d\mathbf{x}, \quad (11)$$

and arbitrarily chosen in $[-\|\beta\|_{L^\infty(\Omega)}, \|\beta\|_{L^\infty(\Omega)}]$ for $m_\nu = 0$, and where the following upwind approximation

$$S_{k, \mathbf{s}}^n = \begin{cases} S_\kappa^n & \text{if } F_{\kappa, \mathbf{s}}(p^n) \geq 0, \\ S_{\mathbf{s}}^n & \text{if } F_{\kappa, \mathbf{s}}(p^n) < 0, \end{cases} \quad (12)$$

of the saturations has been used.

Let us remark that the conservation equations (6), (8) in each cell κ only involve the cell unknowns p_κ and S_κ and the vertex unknowns $p_{\mathbf{s}}$, $S_{\mathbf{s}}$ for all $\mathbf{s} \in \mathcal{V}_\kappa$. It results that, at each iteration of the Newton algorithm used to solve the nonlinear system (6)- (10), the Schur complement of the Jacobian system eliminating the cell unknowns and the cell linearized conservation equations can be computed without any fill-in. It leads to a linear system on the vertex unknowns only with the same stencil than typical P1 or Q1 finite element discretizations. The computation of this Schur complement involves the inversion of a 2 by 2 matrix for each cell and at each Newton iteration which can be shown to be nonsingular for a small enough time step.

3.1 Discrete functional setting

Let $u \in W_{\mathcal{D}}$, we recall that $\pi_{\mathcal{T}}u$ is the piecewise affine function

$$\pi_{\mathcal{T}}u(\mathbf{x}) = \sum_{\nu \in \mathcal{M} \cup \mathcal{V}} u_{\nu} \eta_{\nu}(\mathbf{x}).$$

We define two other function reconstructions from $W_{\mathcal{D}}$ to $L^2(\Omega)$, first the cellwise constant reconstruction

$$\pi_{\mathcal{M}}u(\mathbf{x}) = u_{\kappa} \text{ for all } \mathbf{x} \in \kappa, \kappa \in \mathcal{M},$$

and second the following piecewise constant reconstruction:

$$\pi_{\mathcal{D}}u(\mathbf{x}) = u_{\nu} \text{ for all } \mathbf{x} \in \omega_{\nu}, \nu \in \mathcal{M} \cup \mathcal{V}_{int}.$$

Note that $\pi_{\mathcal{D}}u$ does not depend on the $u_{\mathbf{s}}$ for $\mathbf{s} \in \mathcal{V}_{ext}$.

In the following, for any continuous function $g : \mathbb{R} \rightarrow \mathbb{R}$, and for any $u \in W_{\mathcal{D}}$, the function $g(u) \in W_{\mathcal{D}}$ is defined such that $g(u)_{\kappa} = g(u_{\kappa})$ for all $\kappa \in \mathcal{M}$ and $g(u)_{\mathbf{s}} = g(u_{\mathbf{s}})$ for all $\mathbf{s} \in \mathcal{V}$. Note that we clearly have the properties $\pi_{\mathcal{M}}g(u) = g(\pi_{\mathcal{M}}(u))$ and $\pi_{\mathcal{D}}g(u) = g(\pi_{\mathcal{D}}(u))$.

LEMMA 3.1 For all $u \in W_{\mathcal{D}}$, one has

$$\sum_{\mathbf{s} \in \mathcal{V}_{\kappa}} (v_{\kappa} - v_{\mathbf{s}}) F_{\kappa, \mathbf{s}}(u) = \int_{\kappa} \Lambda(\mathbf{x}) \nabla \pi_{\mathcal{T}}u \cdot \nabla \pi_{\mathcal{T}}v \, d\mathbf{x}, \quad (13)$$

and

$$\underline{\Lambda} \|\nabla \pi_{\mathcal{T}}u\|_{L^2(\kappa)}^2 \leq \sum_{\mathbf{s} \in \mathcal{V}_{\kappa}} (u_{\kappa} - u_{\mathbf{s}}) F_{\kappa, \mathbf{s}}(u) \leq \bar{\Lambda} \|\nabla \pi_{\mathcal{T}}u\|_{L^2(\kappa)}^2.$$

Proof: For all $u \in W_{\mathcal{D}}$, one has by definition of the flux (1)

$$F_{\kappa, \mathbf{s}}(u) = - \int_{\kappa} \Lambda(\mathbf{x}) \nabla \pi_{\mathcal{T}}u \cdot \nabla \eta_{\mathbf{s}} \, d\mathbf{x}.$$

We deduce that for all $u, v \in W_{\mathcal{D}}$

$$\sum_{\mathbf{s} \in \mathcal{V}_{\kappa}} (v_{\kappa} - v_{\mathbf{s}}) F_{\kappa, \mathbf{s}}(u) = \int_{\kappa} \Lambda(\mathbf{x}) \nabla \pi_{\mathcal{T}}u \cdot \nabla \pi_{\mathcal{T}}v \, d\mathbf{x},$$

which yields the lemma from our assumption on Λ . \square

Let ρ_T denote the insphere diameter of T , h_T the diameter of T , and $\mathcal{T}_{\kappa} \subset \mathcal{T}$ the set of tetrahedra of κ . We set $h_{\kappa} = \max_{T \in \mathcal{T}_{\kappa}} h_T$ and $h_{\mathcal{T}} = \max_{T \in \mathcal{T}} h_T$.

We will assume in the convergence analysis that the family of tetrahedral sub-meshes \mathcal{T} is shape regular and that the number of vertices of each cell κ is uniformly bounded. Hence let us set

$$\theta_{\mathcal{T}} = \max_{T \in \mathcal{T}} \frac{h_T}{\rho_T},$$

and

$$\gamma_{\mathcal{M}} = \max_{\kappa \in \mathcal{M}} \#\mathcal{V}_{\kappa}.$$

We have the following lemma.

LEMMA 3.2 There exist $C_1 > 0$ and $C_2 > 0$ depending only on $\gamma_{\mathcal{M}}$ and $\theta_{\mathcal{T}}$ such that, for all $u \in W_{\mathcal{D}}$ and all $\kappa \in \mathcal{M}$, one has

$$C_1 |\kappa| \left(u_{\kappa}^2 + \sum_{\mathbf{s} \in \mathcal{V}_{\kappa}} u_{\mathbf{s}}^2 \right) \leq \|\pi_{\mathcal{T}} u\|_{L^2(\kappa)}^2 \leq C_2 |\kappa| \left(u_{\kappa}^2 + \sum_{\mathbf{s} \in \mathcal{V}_{\kappa}} u_{\mathbf{s}}^2 \right), \quad (14)$$

and

$$C_1 \frac{|\kappa|}{(h_{\kappa})^2} \sum_{\mathbf{s} \in \mathcal{V}_{\kappa}} (u_{\mathbf{s}} - u_{\kappa})^2 \leq \|\nabla \pi_{\mathcal{T}} u\|_{L^2(\kappa)^d}^2 \leq C_2 \frac{|\kappa|}{(h_{\kappa})^2} \sum_{\mathbf{s} \in \mathcal{V}_{\kappa}} (u_{\mathbf{s}} - u_{\kappa})^2. \quad (15)$$

Proof: Let $u(\mathbf{x})$ be a linear function on a tetrahedra $T \in \mathcal{T}_{\kappa}$ of volume $|T|$. We denote by u_i , $i = 0, \dots, 3$, its nodal values at the vertices of T . There exist two reals $D_1 > 0$ and $D_2 > 0$ independent on T and u such that

$$D_1 \|u\|_{L^2(T)}^2 \leq |T| \sum_{i=0}^3 u_i^2 \leq D_2 \|u\|_{L^2(T)}^2, \quad (16)$$

and two reals $E_1 > 0$ and $E_2 > 0$ depending only on $\theta_{\mathcal{T}}$ and independent on u such that

$$E_1 \|\nabla u\|_{L^2(T)^d}^2 \leq \frac{|T|}{(h_T)^2} \sum_{i=1}^3 (u_i - u_0)^2 \leq E_2 \|\nabla u\|_{L^2(T)^d}^2. \quad (17)$$

Let us first mention that the the inequalities (16) and (17) are true for any regular tetrahedron \widehat{T} . Now, let F_T be an affine mapping from \widehat{T} to T . Denoting $\widehat{u} = u \circ F$ one has that

$$|\widehat{T}| \|u\|_{L^2(T)}^2 = |T| \|\widehat{u}\|_{L^2(\widehat{T})}^2,$$

which implies (16) for any T . Let J_T be the Jacobian matrix of the mapping F_T , setting $\|J_T\| = \sup_{\mathbf{x} \neq 0} \frac{|J_T \mathbf{x}|}{|\mathbf{x}|}$ one can show that (see e.g. [10])

$$\|J_T\| \leq \frac{h_T}{\rho_{\widehat{T}}} \quad \text{and} \quad \|J_T^{-1}\| \geq \frac{h_{\widehat{T}}}{\rho_T}.$$

Therefore for any T we have

$$\left(\frac{\rho_{\widehat{T}}}{h_T} \right)^2 |T| \|\nabla \widehat{u}\|_{L^2(\widehat{T})^d}^2 \leq |\widehat{T}| \|\nabla u\|_{L^2(T)^d}^2 \leq \left(\frac{h_{\widehat{T}}}{\rho_T} \right)^2 |T| \|\nabla \widehat{u}\|_{L^2(\widehat{T})^d}^2.$$

Let $u \in W_{\mathcal{D}}$ and $\kappa \in \mathcal{M}$, it results that one has

$$D_1 \|\pi_{\mathcal{T}} u\|_{L^2(\kappa)}^2 \leq \sum_{T=\mathbf{x}_{\kappa} \mathbf{x}_{\sigma} \mathbf{s} \mathbf{s}' \in \mathcal{T}_{\kappa}} |T| \left(u_{\kappa}^2 + u_{\sigma}^2 + u_{\mathbf{s}}^2 + u_{\mathbf{s}'}^2 \right) \leq D_2 \|\pi_{\mathcal{T}} u\|_{L^2(\kappa)}^2.$$

Since there exist $F_1 > 0$ and $F_2 > 0$ depending only on $\gamma_{\mathcal{M}}$ and $\theta_{\mathcal{T}}$ such that $F_1|T| \leq |\kappa| \leq F_2|T|$ for all $T \in \mathcal{T}_{\kappa}$, $\kappa \in \mathcal{M}$ it proves (14) using the convexity estimate $0 \leq u_{\sigma}^2 \leq \sum_{\mathbf{s} \in \mathcal{V}_{\sigma}} \beta_{\sigma, \mathbf{s}} u_{\mathbf{s}}^2 \leq \sum_{\mathbf{s} \in \mathcal{V}_{\sigma}} u_{\mathbf{s}}^2$.

Similarly we have that

$$\begin{aligned} E_1 \|\nabla \pi_{\mathcal{T}} u\|_{L^2(\kappa)^d}^2 &\leq \sum_{T=\mathbf{x}_{\kappa} \mathbf{x}_{\sigma} \mathbf{s} \mathbf{s}' \in \mathcal{T}_{\kappa}} \frac{|T|}{(h_T)^2} \left((u_{\sigma} - u_{\kappa})^2 + (u_{\mathbf{s}} - u_{\kappa})^2 + (u_{\mathbf{s}'} - u_{\kappa})^2 \right) \\ &\leq E_2 \|\nabla \pi_{\mathcal{T}} u\|_{L^2(\kappa)^d}^2 \end{aligned}$$

and $0 \leq (u_{\sigma} - u_{\kappa})^2 \leq \sum_{\mathbf{s} \in \mathcal{V}_{\sigma}} \beta_{\sigma, \mathbf{s}} (u_{\mathbf{s}} - u_{\kappa})^2 \leq \sum_{\mathbf{s} \in \mathcal{V}_{\sigma}} (u_{\mathbf{s}} - u_{\kappa})^2$. Since there exist $G_1 > 0$ and $G_2 > 0$ depending only on $\gamma_{\mathcal{M}}$ and $\theta_{\mathcal{T}}$ such that $G_1 h_{\kappa} \leq h_T \leq G_2 h_{\kappa}$ for all $T \in \mathcal{T}_{\kappa}$, $\kappa \in \mathcal{M}$, it proves (15). \square

LEMMA 3.3 There exist $C_1 > 0$ and $C_2 > 0$ depending only on $\gamma_{\mathcal{M}}$ and $\theta_{\mathcal{T}}$ such that for all $u \in W_{\mathcal{D}}^0$

$$\|\pi_{\mathcal{D}} u\|_{L^2(\Omega)} \leq C_1 \|\pi_{\mathcal{T}} u\|_{L^2(\Omega)} \leq C_2 \|\nabla \pi_{\mathcal{T}} u\|_{L^2(\Omega)^d}. \quad (18)$$

Proof: From the continuous Poincaré inequality and from $\pi_{\mathcal{T}} u \in H_0^1(\Omega)$ there exists C , depending only on the domain Ω , such that for all $u \in W_{\mathcal{D}}^0$

$$\|\pi_{\mathcal{T}} u\|_{L^2(\Omega)} \leq C \|\nabla \pi_{\mathcal{T}} u\|_{L^2(\Omega)^d}.$$

From (14) we deduce that there exists C depending only on $\gamma_{\mathcal{M}}$ and $\theta_{\mathcal{T}}$ such that for all $u \in W_{\mathcal{D}}$

$$\sum_{\kappa \in \mathcal{M}} \left(m_{\kappa}(u_{\kappa})^2 + \sum_{\mathbf{s} \in \mathcal{V}_{\kappa} \cap \mathcal{V}_{int}} m_{\kappa, \mathbf{s}}(u_{\mathbf{s}})^2 \right) \leq \sum_{\kappa \in \mathcal{M}} |\kappa| \left((u_{\kappa})^2 + \sum_{\mathbf{s} \in \mathcal{V}_{\kappa}} (u_{\mathbf{s}})^2 \right) \leq C \|\pi_{\mathcal{T}} u\|_{L^2(\Omega)}^2,$$

which ends the proof of the lemma. \square

LEMMA 3.4 There exists $C > 0$ depending only on $\gamma_{\mathcal{M}}$ and $\theta_{\mathcal{T}}$ such that, for all $u \in W_{\mathcal{D}}$, one has the estimate

$$\|\pi_{\mathcal{D}} u - \pi_{\mathcal{T}} u\|_{L^2(\Omega)} + \|\pi_{\mathcal{D}} u - \pi_{\mathcal{M}} u\|_{L^2(\Omega)} \leq C h_{\mathcal{T}} \|\nabla \pi_{\mathcal{T}} u\|_{L^2(\Omega)^d}. \quad (19)$$

Proof: Using (15), there exists $C > 0$ depending only on $\gamma_{\mathcal{M}}$ and $\theta_{\mathcal{T}}$ such that

$$\begin{aligned} \|\pi_{\mathcal{D}} u - \pi_{\mathcal{M}} u\|_{L^2(\Omega)}^2 &= \sum_{\kappa \in \mathcal{M}} \sum_{\mathbf{s} \in \mathcal{V}_{\kappa} \cap \mathcal{V}_{int}} m_{\kappa, \mathbf{s}} (u_{\mathbf{s}} - u_{\kappa})^2 \\ &\leq \max_{\kappa \in \mathcal{M}} (h_{\kappa})^2 \sum_{\kappa \in \mathcal{M}} \frac{|\kappa|}{(h_{\kappa})^2} \sum_{\mathbf{s} \in \mathcal{V}_{\kappa}} (u_{\mathbf{s}} - u_{\kappa})^2, \\ &\leq C (h_{\mathcal{T}})^2 \|\nabla \pi_{\mathcal{T}} u\|_{L^2(\Omega)^d}^2, \end{aligned}$$

which proves the first part of the inequality. Similarly, using (14) and (15), there exists C depending only on $\gamma_{\mathcal{M}}$ and $\theta_{\mathcal{T}}$, such that

$$\|\pi_{\mathcal{M}} u - \pi_{\mathcal{T}} u\|_{L^2(\Omega)}^2 \leq C \sum_{\kappa \in \mathcal{M}} |\kappa| \sum_{\mathbf{s} \in \mathcal{V}_{\kappa}} (u_{\mathbf{s}} - u_{\kappa})^2 \leq C (h_{\mathcal{T}})^2 \|\nabla \pi_{\mathcal{T}} u\|_{L^2(\Omega)^d}^2.$$

\square

LEMMA 3.5 There exists $C > 0$ depending only on $\gamma_{\mathcal{M}}, \theta_{\mathcal{T}}$ and $\bar{\Lambda}$ such that, for all $u \in W_{\mathcal{D}}$ and for all $\theta_{\kappa, \mathbf{s}} \in \mathbb{R}, \mathbf{s} \in \mathcal{V}_{\kappa}, \kappa \in \mathcal{M}$, one has the estimate

$$\left| \sum_{\kappa \in \mathcal{M}} \sum_{\mathbf{s} \in \mathcal{V}_{\kappa}} \theta_{\kappa, \mathbf{s}} F_{\kappa, \mathbf{s}}(u) \right| \leq C \left(\sum_{\kappa \in \mathcal{M}} \frac{|\kappa|}{h_{\kappa}^2} \sum_{\mathbf{s} \in \mathcal{V}_{\kappa}} \theta_{\kappa, \mathbf{s}}^2 \right)^{1/2} \|\nabla \pi_{\mathcal{T}} u\|_{L^2(\Omega)^d}. \quad (20)$$

Proof: Let us define the function $\theta_{\kappa} = \sum_{\mathbf{s} \in \mathcal{V}_{\kappa}} \theta_{\kappa, \mathbf{s}} \eta_{\mathbf{s}}$, then from (13) and (15) one has the estimates

$$\begin{aligned} \left| \sum_{\mathbf{s} \in \mathcal{V}_{\kappa}} \theta_{\kappa, \mathbf{s}} F_{\kappa, \mathbf{s}}(u) \right| &= \left| \int_{\kappa} \Lambda \nabla \pi_{\mathcal{T}} u \cdot \nabla \theta_{\kappa} d\mathbf{x} \right| \\ &\leq C \|\nabla \pi_{\mathcal{T}} u\|_{L^2(\kappa)^d} \left(\frac{|\kappa|}{h_{\kappa}^2} \sum_{\mathbf{s} \in \mathcal{V}_{\kappa}} \theta_{\kappa, \mathbf{s}}^2 \right)^{1/2}, \end{aligned}$$

from which the Lemma 3.5 is deduced. \square

From the conformity of the VAG discretization and from the compact injection of $H_0^1(\Omega)$ in $L^2(\Omega)$, we can state the following compactness property.

LEMMA 3.6 Let $\mathcal{D}^{(m)}, m \in \mathbb{N}$ be a family of discretizations. Let $u^{(m)} \in W_{\mathcal{D}^{(m)}}^0$, $m \in \mathbb{N}$ be such that $\|\nabla \pi_{\mathcal{T}^{(m)}} u^{(m)}\|_{L^2(\Omega)^d}$ is uniformly bounded. Then, there exists $u \in L^2(\Omega)$ such that, up to a subsequence,

$$\pi_{\mathcal{T}^{(m)}} u^{(m)} \rightarrow u \text{ strongly in } L^2(\Omega);$$

moreover $u \in H_0^1(\Omega)$ and $\nabla \pi_{\mathcal{T}^{(m)}} u^{(m)} \rightharpoonup \nabla u$ weakly in $L^2(\Omega)^d$ along the same subsequence.

We also state the following approximation property which follows from the classical conforming finite element approximation theory and from the fact that the interpolation operator $I_{\sigma}(\psi)$ is exact on affine functions.

LEMMA 3.7 Let $\psi \in C^2(\bar{\Omega})$ and let $\psi_{\mathcal{T}}$ be defined by

$$\psi_{\mathcal{T}}(\mathbf{x}) = \sum_{\nu \in \mathcal{M} \cup \mathcal{V}} \psi(\mathbf{x}_{\nu}) \eta_{\nu}(\mathbf{x}).$$

Then, there exists $C(\psi)$ depending only on $\psi, \gamma_{\mathcal{M}}$ and $\theta_{\mathcal{T}}$, such that

$$\|\psi_{\mathcal{T}} - \psi\|_{H^1(\Omega)} \leq C(\psi) h_{\mathcal{T}}.$$

3.2 A priori estimates

Let us set $W_{\mathcal{D}, \Delta t}^0 = (W_{\mathcal{D}}^0)^N$, and for all $u = (u^n)_{n=1, \dots, N} \in W_{\mathcal{D}, \Delta t}^0$ let us define

$$\begin{aligned} \pi_{\mathcal{D}, \Delta t} u(\mathbf{x}, t) &= \pi_{\mathcal{D}} u^n(\mathbf{x}) \text{ for all } (\mathbf{x}, t) \in \Omega \times (t^{n-1}, t^n], \\ \pi_{\mathcal{M}, \Delta t} u(\mathbf{x}, t) &= \pi_{\mathcal{M}} u^n(\mathbf{x}) \text{ for all } (\mathbf{x}, t) \in \Omega \times (t^{n-1}, t^n], \\ \pi_{\mathcal{T}, \Delta t} u(\mathbf{x}, t) &= \pi_{\mathcal{T}} u^n(\mathbf{x}) \text{ for all } (\mathbf{x}, t) \in \Omega \times (t^{n-1}, t^n]. \end{aligned}$$

PROPOSITION 3.8 (A priori estimates) Let $S, p \in W_{\mathcal{D}, \Delta t}^0$ be a solution of the discrete problem (6) - (10), then it satisfies the estimates

$$\|\pi_{\mathcal{D}, \Delta t} \varphi(S)\|_{L^\infty(0, t_f; L^2(\Omega))} + \|\nabla \pi_{\mathcal{T}, \Delta t} \varphi(S)\|_{L^2(Q_{t_f})^d} + \|\nabla \pi_{\mathcal{T}, \Delta t} p\|_{L^\infty(0, t_f; L^2(\Omega)^d)} \leq C, \quad (21)$$

for C depending only on the data and on $\gamma_{\mathcal{M}}$ and $\theta_{\mathcal{T}}$.

Proof: We first prove the estimate on the discrete pressure. Let $S, p \in W_{\mathcal{D}, \Delta t}^0$ be a solution to the system (6) - (10), for each $n \in \{1, \dots, N\}$ and any $v \in W_{\mathcal{D}}^0$ we define

$$A_{\mathcal{D}}^n(v) = \sum_{\kappa \in \mathcal{M}} \sum_{\mathbf{s} \in \mathcal{V}_\kappa} (v_\kappa - v_{\mathbf{s}}) \lambda(S_\kappa^n) F_{\kappa, \mathbf{s}}(p^n), \quad (22)$$

$$E_{\mathcal{D}}^n(v) = \sum_{\nu \in \mathcal{M} \cup \mathcal{V}_{int}} m_\nu v_\nu (k_\nu^+ + k_\nu^-). \quad (23)$$

Remark that that in view of (6), (7) and (10) one has

$$A_{\mathcal{D}}^n(v) = E_{\mathcal{D}}^n(v) \quad \text{for all } v \in W_{\mathcal{D}}^0. \quad (24)$$

Setting $v = p^n$, we deduce from the definition (11) and from Lemma 3.1 that

$$\int_{\Omega} \pi_{\mathcal{M}} \lambda(S^n) \Lambda(\mathbf{x}) \nabla \pi_{\mathcal{T}} p^n \cdot \nabla \pi_{\mathcal{T}} p^n \, d\mathbf{x} = \frac{1}{\Delta t} \int_{t^{n-1}}^{t^n} \int_{\Omega} \pi_{\mathcal{D}} p^n(\mathbf{x}) (k^+(\mathbf{x}) + k^-(\mathbf{x})) \, d\mathbf{x} dt.$$

Applying the discrete Poincaré inequality given by Lemma 3.3 and taking into account the assumptions on the data, one can establish the estimate on the discrete pressure

$$\|\nabla \pi_{\mathcal{T}, \Delta t} p\|_{L^\infty(0, t_f; L^2(\Omega)^d)} \leq C.$$

Before deriving the estimates on the discrete saturation, let us first introduce some notations. For each $n \in \{1, \dots, N\}$ and any $v \in W_{\mathcal{D}}^0$ we define

$$B_{\mathcal{D}, \Delta t}^n(v) = \sum_{\nu \in \mathcal{M} \cup \mathcal{V}_{int}} \phi_\nu m_\nu v_\nu \frac{S_\nu^n - S_\nu^{n-1}}{\Delta t}, \quad (25)$$

$$C_{\mathcal{D}}^n(v) = \sum_{\kappa \in \mathcal{M}} \sum_{\mathbf{s} \in \mathcal{V}_\kappa} (v_\kappa - v_{\mathbf{s}}) f(S_{\kappa, \mathbf{s}}^n) \lambda(S_\kappa^n) F_{\kappa, \mathbf{s}}(p^n), \quad (26)$$

$$D_{\mathcal{D}}^n(v) = \sum_{\kappa \in \mathcal{M}} \sum_{\mathbf{s} \in \mathcal{V}_\kappa} (v_\kappa - v_{\mathbf{s}}) F_{\kappa, \mathbf{s}}(\varphi(S^n)), \quad (27)$$

$$F_{\mathcal{D}}^n(v) = \sum_{\nu \in \mathcal{M} \cup \mathcal{V}_{int}} m_\nu v_\nu k_\nu^{o, n}. \quad (28)$$

It follows from (8), (9) and (10) that

$$B_{\mathcal{D}, \Delta t}^n(v) + C_{\mathcal{D}}^n(v) + D_{\mathcal{D}}^n(v) = F_{\mathcal{D}}^n(v) \quad \text{for all } v \in W_{\mathcal{D}}^0. \quad (29)$$

Actually, for a given S^{n-1} the variational problem (24)-(29) is equivalent to (6) - (10).

Let us first estimate $\sum_{n=1}^m \Delta t B_{\mathcal{D}, \Delta t}^n(\varphi(S^n))$ for $m \in \{1, \dots, N\}$, we remark that defining

$$\Phi(S) = \int_0^S \varphi(\tau) \, d\tau \text{ for all } S \in \mathbb{R},$$

one has

$$\frac{1}{2L_\varphi}(\varphi(S))^2 \leq \Phi(S) \leq \frac{L_\varphi}{2} S^2, \quad (30)$$

where L_φ is the Lipschitz constant of the function φ (cf. Lemma 11.7 of [5]). We have that

$$\Phi(a) - \Phi(b) = \varphi(a)(a - b) + \int_b^a (\varphi(\tau) - \varphi(a)) \, d\tau \text{ for all } a, b \in \mathbb{R}.$$

Thus, in view of the monotonicity of φ , the last term in the above inequality is non positive so that

$$\begin{aligned} \sum_{n=1}^m \Delta t B_{\mathcal{D}, \Delta t}^n(\varphi(S^n)) &\geq \sum_{n=1}^m \sum_{\nu \in \text{MU}\mathcal{V}_{int}} \phi_\nu m_\nu (\Phi(S_\nu^n) - \Phi(S_\nu^{n-1})) \\ &\geq \sum_{\nu \in \text{MU}\mathcal{V}_{int}} \phi_\nu m_\nu (\Phi(S_\nu^m) - \Phi(S_\nu^0)), \end{aligned}$$

which leads, using (30), to

$$\sum_{n=1}^m \Delta t B_{\mathcal{D}, \Delta t}^n(\varphi(S^n)) \geq \frac{1}{2L_\varphi} \sum_{\nu \in \text{MU}\mathcal{V}_{int}} \phi_\nu m_\nu (\varphi(S_\nu^m))^2 - \frac{L_\varphi}{2} \sum_{\nu \in \text{MU}\mathcal{V}_{int}} \phi_\nu m_\nu (S_\nu^0)^2$$

and then to

$$\sum_{n=1}^m \Delta t B_{\mathcal{D}, \Delta t}^n(\varphi(S^n)) \geq \frac{\phi}{2L_\varphi} \|\pi_{\mathcal{D}} \varphi(S^m)\|_{L^2(\Omega)}^2 - \frac{\bar{\phi} L_\varphi}{2} \|\pi_{\mathcal{D}} S^0\|_{L^2(\Omega)}^2 \quad (31)$$

in view of assumption \mathcal{H}_1 .

Next, applying Lemma 3.5 with $u = p^n$ and $\theta_{\kappa, \mathbf{s}}^n = (\varphi(S_\kappa^n) - \varphi(S_\mathbf{s}^n)) f(S_{\kappa, \mathbf{s}}^n) \lambda(S_\kappa^n)$ one can derive that

$$\sum_{n=1}^m \Delta t C_{\mathcal{D}}^n(\varphi(S^n)) \leq C \|\nabla \pi_{\mathcal{T}, \Delta t} p\|_{L^2(Q_{t_f})^d} \left(\sum_{n=1}^m \Delta t \sum_{\kappa \in \mathcal{M}} \frac{|\kappa|}{h_\kappa^2} \sum_{\mathbf{s} \in \mathcal{V}_\kappa} (\theta_{\kappa, \mathbf{s}}^n)^2 \right)^{1/2}.$$

Using the boundedness of f and λ , (15), and the estimate on the discrete pressure, we deduce that

$$\sum_{n=1}^m \Delta t C_{\mathcal{D}}^n(\varphi(S^n)) \leq C \|\nabla \pi_{\mathcal{T}, \Delta t} \varphi(S)\|_{L^2(Q_{t_f})^d}. \quad (32)$$

It follows from Lemma 3.1 that

$$\sum_{n=1}^m \Delta t D_{\mathcal{D}}^n(\varphi(S^n)) \geq \underline{\Delta} \|\nabla \pi_{\mathcal{T}, \Delta t} \varphi(S)\|_{L^2(Q_{t_f})^d}^2. \quad (33)$$

Applying the Cauchy-Schwarz inequality to $\sum_{n=1}^m \Delta t F_{\mathcal{D}}^n(\varphi(S^n))$ we obtain

$$\sum_{n=1}^m \Delta t F_{\mathcal{D}}^n(\varphi(S^n)) \leq \|\pi_{\mathcal{D}, \Delta t} k^{o,n}\|_{L^2(Q_{t_f})} \|\pi_{\mathcal{D}, \Delta t} \varphi(S)\|_{L^2(Q_{t_f})}.$$

Thus, from Lemma 3.3, the assumption \mathcal{H}_6 , and the boundedness of f , we deduce that there exists some positive C such that

$$\sum_{n=1}^m \Delta t F_{\mathcal{D}}^n(\varphi(S^n)) \leq C \|\nabla \pi_{\mathcal{T}, \Delta t} \varphi(S)\|_{L^2(Q_{t_f})^d}. \quad (34)$$

Gathering (31), (32), (33) and (34), and using the Young inequality, the proof is completed. \square

From Proposition 3.8 we deduce the following existence result for the discrete solution which can be proven by a simple adaptation of Theorem 12.2 of [5] based on a topological degree argument.

LEMMA 3.9 The discrete problem (6) - (10) has at least one solution.

LEMMA 3.10 (A priori estimates in dual norm) Let $S, p \in W_{\mathcal{D}, \Delta t}^0$ be a solution of the discrete problem (6) - (10), then there exists C depending only on $\gamma_{\mathcal{M}}$, $\theta_{\mathcal{T}}$ and on the data such that

$$\sum_{n=1}^N \frac{1}{\Delta t} \|S^n - S^{n-1}\|_{-1,2,\mathcal{T}}^2 \leq C, \quad (35)$$

where the norm $\|\cdot\|_{-1,2,\mathcal{T}}$ is defined by

$$\|v\|_{-1,2,\mathcal{T}} = \sup_{w \in W_{\mathcal{D}}^0, w \neq 0} \frac{1}{\|\nabla \pi_{\mathcal{T}} w\|_{L^2(\Omega)^d}} \sum_{\nu \in \mathcal{M} \cup \mathcal{V}_{int}} m_{\nu} v_{\nu} w_{\nu} \quad \text{for all } v \in W_{\mathcal{D}}^0.$$

Proof: Let $\psi \in W_{\mathcal{D}}^0$, using the notations of Proposition 3.8, we deduce from Lemma 3.5 the following inequality

$$|C_{\mathcal{D}}^n(\psi)| \leq C \left(\sum_{\kappa \in \mathcal{M}} \sum_{s \in \mathcal{V}_{\kappa}} \frac{|\kappa|}{(h_{\kappa})^2} f(S_{\kappa,s}^n)^2 \lambda^2(S_{\kappa}^n) (\psi_s - \psi_{\kappa})^2 \right)^{\frac{1}{2}} \|\nabla \pi_{\mathcal{T}} p^n\|_{L^2(\Omega)^d}.$$

In view of (21), and since f and λ are bounded, we obtain

$$|C_{\mathcal{D}}^n(\psi)| \leq C \|\nabla \pi_{\mathcal{T}} \psi\|_{L^2(\Omega)^d}.$$

Thanks to (13) and our assumption on $\Lambda(\mathbf{x})$ one has

$$|D_{\mathcal{D}}^n(\psi)| \leq \bar{\Lambda} \|\nabla \pi_{\mathcal{T}} \psi\|_{L^2(\Omega)^d} \|\nabla \pi_{\mathcal{T}} \varphi(S^n)\|_{L^2(\Omega)^d}.$$

Next, it follows from the Cauchy-Schwarz inequality, the boundedness of f and Lemma 3.3 inequality that there exists C depending only on $\gamma_{\mathcal{M}}$ and $\theta_{\mathcal{T}}$ such that

$$|F_{\mathcal{D}}^n(\psi)| \leq C \|\nabla \pi_{\mathcal{T}} \psi\|_{L^2(\Omega)^d}.$$

Thus, in view of (29) and of (5)

$$\frac{\phi}{\nu} \sum_{\nu \in \mathcal{M} \cup \mathcal{V}_{int}} m_\nu (S_\nu^n - S_\nu^{n-1}) \psi_\nu \leq C \Delta t \left(1 + \|\nabla \pi_{\mathcal{T}} \varphi(S^n)\|_{L^2(\Omega)^d} \right) \|\nabla \pi_{\mathcal{T}} \psi\|_{L^2(\Omega)^d}$$

and

$$\|S^n - S^{n-1}\|_{-1,2,\mathcal{T}} \leq C \Delta t \left(1 + \|\nabla \pi_{\mathcal{T}} \varphi(S^n)\|_{L^2(\Omega)^d} \right),$$

which in turn implies (35) thanks to (21). \square

LEMMA 3.11 Let $S, p \in W_{\mathcal{D}, \Delta t}^0$ be a solution of the discrete problem (6) - (10), then there exists C depending only on $\gamma_{\mathcal{M}}$, $\theta_{\mathcal{T}}$ and the data such that

$$\int_0^{t_f - \tau} \int_{\Omega} (\pi_{\mathcal{D}, \Delta t} \varphi(S)(\cdot, \cdot + \tau) - \pi_{\mathcal{D}, \Delta t} \varphi(S))^2 \, d\mathbf{x} dt \leq C \tau \quad \text{for all } \tau > 0. \quad (36)$$

Proof: Let $\lceil s \rceil$ denotes the smallest integer larger or equal to s , we set $n_{\Delta t}(t) = \lceil t/\Delta t \rceil$ for all $t \in [0, t_f]$. In view of \mathcal{H}_1 , we have that

$$\begin{aligned} & \int_0^{t_f - \tau} \int_{\Omega} (\pi_{\mathcal{D}, \Delta t} \varphi(S)(\cdot, \cdot + \tau) - \pi_{\mathcal{D}, \Delta t} \varphi(S))^2 \, d\mathbf{x} dt \leq \\ & \leq L_\varphi \int_0^{t_f - \tau} \sum_{\nu \in \mathcal{M} \cup \mathcal{V}_{int}} m_\nu \left(\varphi(S_\nu^{n_{\Delta t}(t+\tau)}) - \varphi(S_\nu^{n_{\Delta t}(t)}) \right) \cdot \sum_{k=n_{\Delta t}(t)+1}^{n_{\Delta t}(t+\tau)} (S_\nu^k - S_\nu^{k-1}) \, dt \end{aligned} \quad (37)$$

For all $\xi \in [0, \tau]$ we define

$$T_\xi(\tau) = \int_0^{t_f - \tau} \sum_{k=n_{\Delta t}(t)+1}^{n_{\Delta t}(t+\tau)} \sum_{\nu \in \mathcal{M} \cup \mathcal{V}_{int}} m_\nu \varphi(S_\nu^{n_{\Delta t}(t+\xi)}) (S_\nu^k - S_\nu^{k-1}) \, dt$$

such that

$$\begin{aligned} T_\xi(\tau) & \leq \int_0^{t_f - \tau} \sum_{k=n_{\Delta t}(t)+1}^{n_{\Delta t}(t+\tau)} \|\nabla \pi_{\mathcal{T}} \varphi(S^{n_{\Delta t}(t+\xi)})\|_{L^2(\Omega)^d} \|S_\nu^k - S_\nu^{k-1}\|_{-1,2,\mathcal{T}} \, dt \\ & \leq \frac{1}{2} \int_0^{t_f - \tau} \sum_{k=n_{\Delta t}(t)+1}^{n_{\Delta t}(t+\tau)} \Delta t \|\nabla \pi_{\mathcal{T}} \varphi(S^{n_{\Delta t}(t+\xi)})\|_{L^2(\Omega)^d}^2 \, dt \\ & \quad + \frac{1}{2} \int_0^{t_f - \tau} \sum_{k=n_{\Delta t}(t)+1}^{n_{\Delta t}(t+\tau)} \frac{1}{\Delta t} \|S_\nu^k - S_\nu^{k-1}\|_{-1,2,\mathcal{T}}^2 \, dt. \end{aligned}$$

It follows from Lemma 6.1 and 6.2 of [1] that

$$T_\xi(\tau) \leq \frac{\tau}{2} \sum_{k=1}^N \Delta t \|\nabla \pi_{\mathcal{T}} \varphi(S^k)\|_{L^2(\Omega)^d}^2 + \frac{\tau}{2} \sum_{k=1}^N \frac{1}{\Delta t} \|S^k - S^{k-1}\|_{-1,2,\mathcal{T}}^2.$$

Thus, in view of Proposition 3.8 and Lemma 3.10 we have that $T_\xi(\tau) \leq C\tau$ for all $\xi \in [0, \tau]$, where C depends only on $\gamma_{\mathcal{M}}$, $\theta_{\mathcal{T}}$ and on the data. To complete the proof, it suffices to notice that the right-hand-side of inequality (37) is equal to $T_\tau(\tau) - T_0(\tau)$. \square

3.3 Convergence proof

This section is devoted to the proof of the following theorem.

THEOREM 3.12 (Main result) Let $(\mathcal{D}^{(m)})_{m \in \mathbb{N}}$ be a sequence of discretizations of Ω such that there exist two positive constants θ and γ satisfying $\theta_{\mathcal{T}^{(m)}} \leq \theta$, $\gamma_{\mathcal{M}^{(m)}} \leq \gamma$ for all $m \in \mathbb{N}$, and such that $h_{\mathcal{T}^{(m)}} \rightarrow 0$ as $m \rightarrow \infty$. Let $\Delta t^{(m)}$ be a sequence of real positive numbers, such that $t_f / \Delta t^{(m)} \in \mathbb{N}$ for all $m \in \mathbb{N}$ and such that $\Delta t^{(m)} \rightarrow 0$ as $m \rightarrow \infty$. Let $(S^{(m)}, p^{(m)})_{m \in \mathbb{N}}$ be a corresponding sequence of approximate solutions. Then, there exist $\bar{S} \in L^\infty(0, t_f; L^2(\Omega))$, $\bar{p} \in L^\infty(0, t_f; H_0^1(\Omega))$ and a subsequence of $(S^{(m)}, p^{(m)})_{m \in \mathbb{N}}$, which we denote again by $(S^{(m)}, p^{(m)})_{m \in \mathbb{N}}$, such that

$$\pi_{\mathcal{D}^{(m)} \Delta t^{(m)}} S^{(m)}, \pi_{\mathcal{M}^{(m)} \Delta t^{(m)}} S^{(m)} \rightarrow \bar{S} \text{ strongly in } L^2(Q_{t_f}) \text{ as } m \rightarrow \infty$$

and

$$\pi_{\mathcal{T}^{(m)} \Delta t^{(m)}} p^{(m)} \rightharpoonup \bar{p} \text{ weakly in } L^2(Q_{t_f}) \text{ as } m \rightarrow \infty;$$

moreover $\varphi(\bar{S}) \in L^2(0, t_f; H_0^1(\Omega))$ and (\bar{S}, \bar{p}) verifies the system (2) in the weak sense (3).

To begin with, we prove a compactness and the regularity of the limit of the sequences $\pi_{\mathcal{T}^{(m)} \Delta t^{(m)}} \varphi(S^{(m)})$ and $\pi_{\mathcal{M}^{(m)} \Delta t^{(m)}} p^{(m)}$.

LEMMA 3.13 There exists $\bar{S} \in L^2(Q_{t_f})$ such that $\varphi(\bar{S}) \in L^2(0, t_f; H_0^1(\Omega))$ and up to a subsequence,

$$\pi_{\mathcal{T}^{(m)} \Delta t^{(m)}} \varphi(S^{(m)}) \rightarrow \varphi(\bar{S}) \text{ strongly in } L^2(Q_{t_f}) \text{ as } m \rightarrow +\infty,$$

and

$$\nabla \pi_{\mathcal{T}^{(m)} \Delta t^{(m)}} \varphi(S^{(m)}) \rightharpoonup \nabla \varphi(\bar{S}) \text{ weakly in } L^2(Q_{t_f})^d \text{ as } m \rightarrow +\infty.$$

Moreover $\pi_{\mathcal{D}^{(m)} \Delta t^{(m)}} S^{(m)}$ and $\pi_{\mathcal{M}^{(m)} \Delta t^{(m)}} S^{(m)}$ converge to \bar{S} strongly in $L^2(Q_{t_f})$ as $m \rightarrow +\infty$ up to the same subsequence.

Proof: Extending $\pi_{\mathcal{T}^{(m)} \Delta t^{(m)}} \varphi(S^{(m)})$ by zero outside of Q_{t_f} we deduce from (21), (36) and (19) that there exists C depending only on γ , θ and on the data such

$$\|\pi_{\mathcal{T}^{(m)} \Delta t^{(m)}} \varphi(S^{(m)}) (\cdot, \cdot + \tau) - \pi_{\mathcal{T}^{(m)} \Delta t^{(m)}} \varphi(S^{(m)})\|_{L^2(\mathbb{R}^{d+1})} \leq C(\tau + h_{\mathcal{T}^{(m)}})$$

and therefore using Lemma B.2 of [11] we have that

$$\limsup_{\tau \rightarrow 0} \sup_{m \in \mathbb{N}} \left\{ \|\pi_{\mathcal{T}^{(m)} \Delta t^{(m)}} \varphi(S^{(m)}) (\cdot, \cdot + \tau) - \pi_{\mathcal{T}^{(m)} \Delta t^{(m)}} \varphi(S^{(m)})\|_{L^2(\mathbb{R}^{d+1})} \right\} = 0.$$

Since, from the a priori estimate (21), the sequence $\pi_{\mathcal{T}^{(m)} \Delta t^{(m)}} \varphi(S^{(m)})$ is also uniformly bounded in $L^2(\mathbb{R}; H_0^1(\mathbb{R}^d))$, we deduce from the Fréchet-Kolmogorov Theorem that the sequence $(\pi_{\mathcal{T}^{(m)} \Delta t^{(m)}} \varphi(S^{(m)}))_{m \in \mathbb{N}}$ is relatively compact in $L^2(\mathbb{R}^{d+1})$ (and also in $L^2(Q_{t_f})$). Therefore, there exists some function $\Phi \in L^2(Q_{t_f})$ such that up to a subsequence $\pi_{\mathcal{T}^{(m)} \Delta t^{(m)}} \varphi(S^{(m)}) \rightarrow \Phi$ strongly in $L^2(\mathbb{R}^{d+1})$ (and also in $L^2(Q_{t_f})$).

On the other hand, a simple adaptation of Lemma 3.6 to the time-dependent setting allows to conclude that

$$\Phi \in L^2(0, t_f; H_0^1(\Omega)) \quad \text{and} \quad \nabla \pi_{\mathcal{T}^{(m)} \Delta t^{(m)}} \varphi \left(S^{(m)} \right) \rightharpoonup \nabla \Phi \text{ weakly in } L^2(Q_{t_f})^d,$$

as $m \rightarrow \infty$ up to the same subsequence.

It remains to show that $\pi_{\mathcal{D}^{(m)} \Delta t^{(m)}} S^{(m)}$ and $\pi_{\mathcal{M}^{(m)} \Delta t^{(m)}} S^{(m)}$ converge strongly to $\bar{S} := \varphi^{-1}(\Phi)$. Let us first remark that $\pi_{\mathcal{D}^{(m)} \Delta t^{(m)}} \varphi \left(S^{(m)} \right)$ and $\pi_{\mathcal{M}^{(m)} \Delta t^{(m)}} \varphi \left(S^{(m)} \right)$ converges in $L^2(Q_{t_f})$ to $\varphi(\bar{S})$ along the same subsequence as $\pi_{\mathcal{T}^{(m)} \Delta t^{(m)}} \varphi \left(S^{(m)} \right)$ thanks to (19) and (21). Next, in view of the assumptions \mathcal{H}_1 and \mathcal{H}_7 the function φ^{-1} belongs to $C(\mathbb{R})$ and satisfies

$$|\varphi^{-1}(u)| \leq 1 + L_\varphi^{-1}|u|. \tag{38}$$

Therefore, one can deduce (cf. [1, Lemma 7.1]) that, up to a subsequence,

$$\pi_{\mathcal{D}^{(m)} \Delta t^{(m)}} S^{(m)}, \pi_{\mathcal{M}^{(m)} \Delta t^{(m)}} S^{(m)} \rightarrow \bar{S} = \varphi^{-1}(\Phi) \quad \text{strongly in } L^2(Q_{t_f}).$$

□

From Lemma 3.6 and Proposition 3.8 we can state the following Lemma.

LEMMA 3.14 There exists $\bar{p} \in L^\infty(0, t_f; H_0^1(\Omega))$ such that, up to a subsequence,

$$\pi_{\mathcal{T}^{(m)} \Delta t^{(m)}} p^{(m)} \rightharpoonup \bar{p} \text{ weakly in } L^2(Q_{t_f}) \text{ as } m \rightarrow +\infty.$$

Moreover, $(\nabla \pi_{\mathcal{T}^{(m)} \Delta t^{(m)}} p^{(m)})_m$ converges weakly in $L^2(Q_{t_f})^d$ to $\nabla \bar{p}$ along the same subsequence.

Finally we prove that the function pair (\bar{S}, \bar{p}) is a weak solution in the sense of (3). For this purpose we introduce the function space

$$\Psi = \{\psi \in C^{2,1}(\bar{\Omega} \times [0, t_f]), \quad \psi = 0 \text{ on } \partial\Omega \times [0, t_f], \quad \psi(\cdot, t_f) = 0\}.$$

For any $\bar{\psi} \in \Psi$ we define its projection on the discrete space $W_{\mathcal{D}, \Delta t}^0$ by $\psi_\nu^n = \psi(\mathbf{x}_\nu, t_n)$ for all $\nu \in \mathcal{M} \cup \mathcal{V}$; the corresponding projection of $\bar{\psi}$ onto the finite element space $V_{\mathcal{T}}$ is denoted by $\pi_{\mathcal{T}, \Delta t} \bar{\psi}$.

We recall that for all $n \in \{1, \dots, N\}$ the system (6)-(10) can be written in the following variational form

$$\begin{aligned} A_{\mathcal{D}}^n(v) &= E_{\mathcal{D}}^n(v) && \text{for all } v \in W_{\mathcal{D}}^0, \\ B_{\mathcal{D}, \Delta t}^n(v) + C_{\mathcal{D}}^n(v) + D_{\mathcal{D}}^n(v) &= F_{\mathcal{D}}^n(v) && \text{for all } v \in W_{\mathcal{D}}^0, \end{aligned}$$

where $A_{\mathcal{D}}^n(v)$, $E_{\mathcal{D}}^n(v)$, $B_{\mathcal{D}, \Delta t}^n(v)$, $C_{\mathcal{D}}^n(v)$, $D_{\mathcal{D}}^n(v)$, $F_{\mathcal{D}}^n(v)$ have been defined in respectively equations (22), (23), (25), (26), (27), (28). In particular we have that

$$\begin{aligned} \sum_{n=1}^N \Delta t A_{\mathcal{D}}^n(\psi^{n-1}) &= \sum_{n=1}^N \Delta t E_{\mathcal{D}}^n(\psi^{n-1}), \\ \sum_{n=1}^N \Delta t B_{\mathcal{D}, \Delta t}^n(\psi^{n-1}) + \sum_{n=1}^N \Delta t C_{\mathcal{D}}^n(\psi^{n-1}) + \sum_{n=1}^N \Delta t D_{\mathcal{D}}^n(\psi^{n-1}) &= \sum_{n=1}^N \Delta t F_{\mathcal{D}}^n(\psi^{n-1}). \end{aligned} \tag{39}$$

For each of the term in (39) we will prove a corresponding convergence result.

Accumulation term We consider the term $\sum_{n=1}^N \Delta t B_{\mathcal{D}, \Delta t}^n(\psi^{n-1})$. Applying the chain rule and using the fact that $\bar{\psi}(x, T) = 0$ we obtain

$$\begin{aligned} \sum_{n=1}^N \Delta t B_{\mathcal{D}, \Delta t}^n(\psi^{n-1}) &= - \sum_{n=1}^N \sum_{\nu \in \mathcal{M} \cup \mathcal{V}_{int}} \int_{t_{n-1}}^{t_n} \int_{\omega_\nu} \phi(\mathbf{x}) \pi_{\mathcal{D}, \Delta t} S(\mathbf{x}, t) \partial_t \bar{\psi}(\mathbf{x}_\nu, t) \, d\mathbf{x} dt \\ &\quad - \sum_{\nu \in \mathcal{M} \cup \mathcal{V}_{int}} \int_{\omega_\nu} \phi(\mathbf{x}) \bar{\psi}(\mathbf{x}_\nu, 0) S_0(\mathbf{x}) \, d\mathbf{x}. \end{aligned}$$

The proof of the fact that

$$\sum_{n=1}^N \Delta t B_{\mathcal{D}, \Delta t}^n(\psi^{n-1}) \rightarrow - \int_{\Omega} \int_0^{t_f} \phi(\mathbf{x}) \bar{S}(\mathbf{x}, t) \partial_t \bar{\psi}(\mathbf{x}, t) \, d\mathbf{x} dt - \int_{\Omega} \phi(\mathbf{x}) \bar{\psi}(\mathbf{x}, 0) S_0(\mathbf{x}) \, d\mathbf{x}$$

is classical since in view of Lemma 3.13 the function $\pi_{\mathcal{D}, \Delta t} S$ tends to \bar{S} strongly in $L^2(Q_{t_f})$.

Diffusion terms It follows from (22) and (13) that

$$\sum_{n=1}^N \Delta t A_{\mathcal{D}}^n(\psi^{n-1}) = \int_0^{t_f} \int_{\Omega} \lambda(\pi_{\mathcal{M}, \Delta t} S(\mathbf{x}, t)) \Lambda(\mathbf{x}) \nabla \pi_{\mathcal{T}, \Delta t} p(\mathbf{x}, t) \cdot \nabla \pi_{\mathcal{T}, \Delta t} \psi(\mathbf{x}, t - \Delta t) \, d\mathbf{x} dt.$$

Hence,

$$\sum_{n=1}^N \Delta t A_{\mathcal{D}}^n(\psi^{n-1}) \rightarrow \int_0^{t_f} \int_{\Omega} \lambda(S(\mathbf{x}, t)) \Lambda(\mathbf{x}) \nabla \bar{p}(\mathbf{x}, t) \cdot \nabla \psi(\mathbf{x}, t) \, d\mathbf{x} dt$$

in view of Lemmae 3.13, 3.14 and 3.7. Similarly one can show that

$$\sum_{n=1}^N \Delta t D_{\mathcal{D}}^n(\psi^{n-1}) \rightarrow \int_0^{t_f} \int_{\Omega} \Lambda(\mathbf{x}) \nabla \varphi(\bar{S}(\mathbf{x}, t)) \cdot \nabla \psi(\mathbf{x}, t) \, d\mathbf{x} dt$$

using lemmae 3.13 and 3.7.

Convection term For each cell $\kappa \in \mathcal{M}$ let $(V_{\kappa, \mathbf{s}})_{\mathbf{s} \in \mathcal{V}_\kappa}$ be some partition of κ such that $|\kappa| = \sum_{\mathbf{s} \in \mathcal{V}_\kappa} \int_{V_{\kappa, \mathbf{s}}} d\mathbf{x}$ and $|V_{\kappa, \mathbf{s}}| = \int_{V_{\kappa, \mathbf{s}}} d\mathbf{x} > 0$. For all $\kappa \in \mathcal{M}$ and $\mathbf{s} \in \mathcal{V}_\kappa$ we set

$$T_{\kappa, \mathbf{s}}^n = \frac{1}{|V_{\kappa, \mathbf{s}}|} (\psi_\kappa^{n-1} - \psi_{\mathbf{s}}^{n-1}) \lambda(S_\kappa^n) F_{\kappa, \mathbf{s}}(p^n), \quad (40)$$

and we define a piecewise constant function $T_V \in L^2(Q_{t_f})$ such that $T_V(\mathbf{x}, t) = T_{\kappa, \mathbf{s}}^n$ for all $x \in V_{\kappa, \mathbf{s}}, t \in (t_{n-1}, t_n)$. We also define the function S_V , such that $S_V(\mathbf{x}, t) = S_{\kappa, \mathbf{s}}^n$ for $x \in V_{\kappa, \mathbf{s}}$ and $t \in (t_{n-1}, t_n)$. Therefore, the convection term can be written as

$$\sum_{n=1}^N \Delta t C_{\mathcal{D}}^n(\psi^{n-1}) = \int_0^{t_f} \int_{\Omega} T_V f(S_V) \, d\mathbf{x} dt.$$

Let us first remark that $f(S_V) \rightarrow f(\bar{S})$ strongly in $L^2(Q_{t_f})$. Indeed, using the same type of estimates that in the proof of Lemma 3.4 one shows that $\varphi(S_V) \rightarrow \varphi(\bar{S})$ strongly in $L^2(Q_{t_f})$, which yields the convergence of S_V in view of (38). Hence, $f(S_V) \rightarrow f(\bar{S})$ thanks to the assumption \mathcal{H}_2 . We will show below that $T_V \rightharpoonup \lambda(\bar{S})\Lambda\nabla\bar{p} \cdot \nabla\psi$ weakly in $L^2(Q_{t_f})$. For all $\xi \in \Psi$ we have

$$\int_0^{t_f} \int_{\Omega} T_V \xi \, d\mathbf{x} = T_1 + T_2,$$

with

$$T_1 = \sum_{n=1}^N \sum_{\kappa \in \mathcal{M}} \sum_{\mathbf{s} \in \mathcal{V}_{\kappa}} \int_{t_{n-1}}^{t_n} \int_{V_{\kappa,\mathbf{s}}} T_{\kappa,\mathbf{s}}^n (\xi - \xi(\mathbf{x}_{\kappa}, t_n)) \, d\mathbf{x} dt$$

and

$$T_2 = \sum_{n=1}^N \sum_{\kappa \in \mathcal{M}} \sum_{\mathbf{s} \in \mathcal{V}_{\kappa}} \int_{t_{n-1}}^{t_n} \int_{V_{\kappa,\mathbf{s}}} T_{\kappa,\mathbf{s}}^n \xi(\mathbf{x}_{\kappa}, t_n) \, d\mathbf{x} dt.$$

From (40) and (13) we deduce that

$$T_2 = \int_0^{t_f} \int_{\Omega} \xi_{\mathcal{M},\Delta t}(\mathbf{x}, t) \lambda(\pi_{\mathcal{M},\Delta t} S(\mathbf{x}, t)) \Lambda(\mathbf{x}) \nabla \pi_{\mathcal{T},\Delta t} p(\mathbf{x}, t) \cdot \nabla \pi_{\mathcal{T},\Delta t} \psi(\mathbf{x}, t - \Delta t) \, d\mathbf{x} dt,$$

where $\xi_{\mathcal{M},\Delta t}$ is a cellwise constant function defined by $\xi_{\mathcal{M},\Delta t} = \xi(\mathbf{x}_{\kappa}, t_n)$ for all $\mathbf{x} \in \kappa$ and $t \in (t_{n-1}, t_n)$. Since $\nabla \pi_{\mathcal{T},\Delta t} p(\mathbf{x}, t)$ tends to $\nabla \bar{p}$ weakly in $L^2(Q_{t_f})^d$, $\xi_{\mathcal{M},\Delta t}$ tends to ξ strongly in $L^\infty(Q_{t_f})$, $\nabla \pi_{\mathcal{T},\Delta t} \psi(\cdot, \cdot - \Delta t)$ tends to $\nabla \psi$ strongly in $L^\infty(Q_{t_f})^d$, and $\lambda(\pi_{\mathcal{M},\Delta t} S)$ tends to $\lambda(\bar{S})$ strongly in $L^2(Q_{t_f})$, we deduce that T_2 tends to $\int_0^{t_f} \int_{\Omega} \xi \lambda(\bar{S}) \Lambda \nabla \bar{p} \cdot \nabla \psi \, d\mathbf{x} dt$ as $h_{\mathcal{T}}, \Delta t$ go to zero. On the other hand, setting

$$\Xi_{\kappa,\mathbf{s}}^n = \frac{1}{\Delta t |V_{\kappa,\mathbf{s}}|} \int_{t_{n-1}}^{t_n} \int_{V_{\kappa,\mathbf{s}}} \xi \, d\mathbf{x} dt - \xi(\mathbf{x}_{\kappa}, t_n)$$

we obtain that

$$T_1 = \sum_{n=1}^N \Delta t \sum_{\kappa \in \mathcal{M}} \sum_{\mathbf{s} \in \mathcal{V}_{\kappa}} (\psi_{\kappa}^{n-1} - \psi_{\mathbf{s}}^{n-1}) \lambda(S_{\kappa}^n) F_{\kappa,\mathbf{s}}(p^n) \Xi_{\kappa,\mathbf{s}}^n.$$

In view of Lemma 3.5 there exists a positive constant C_1 independent of h_{κ} and Δt such that

$$|T_1|^2 \leq C \left(\sum_{n=1}^N \Delta t \sum_{\kappa \in \mathcal{M}} \sum_{\mathbf{s} \in \mathcal{V}_{\kappa}} \frac{|\kappa|}{h_{\kappa}^2} (\psi_{\kappa}^{n-1} - \psi_{\mathbf{s}}^{n-1})^2 \lambda(S_{\kappa}^n)^2 (\Xi_{\kappa,\mathbf{s}}^n)^2 \right) \|\nabla \pi_{\mathcal{T},\Delta t} p\|_{L^2(Q_{t_f})^d}^2.$$

Thanks to the regularity of ξ and ψ there exists a positive constant C_2 such that

$$|\Xi_{\kappa,\mathbf{s}}^n| \leq C(h_{\kappa} + \Delta t) \quad \text{and} \quad |\psi_{\kappa}^{n-1} - \psi_{\mathbf{s}}^{n-1}| \leq C h_{\kappa}.$$

which implies $\lim_{h_{\mathcal{T}}, \Delta t \rightarrow 0} T_1 = 0$ in view of inequality (21) and assumptions \mathcal{H}_2 and \mathcal{H}_7 .

Source term In view of (11), the assumption \mathcal{H}_6 and using the regularity of ϕ we deduce that

$$\begin{aligned} E_{\mathcal{D}}^n(\psi^{n-1}) &= \sum_{n=1}^N \int_{t_{n-1}}^{t_n} \int_{\Omega} \pi_{\mathcal{D},\Delta t} \psi(\mathbf{x}, t_{n-1}) (k^+(\mathbf{x}) + k^-(\mathbf{x})) \, d\mathbf{x} dt \\ &\rightarrow \int_0^{t_f} \int_{\Omega} \bar{\psi}(\mathbf{x}, t) (k^+(\mathbf{x}) + k^-(\mathbf{x})) \, d\mathbf{x} dt \quad \text{as } h_{\mathcal{T}}, \Delta t \rightarrow 0. \end{aligned}$$

Similarly, let us set $k_{\mathcal{D},\Delta t}^o = f(\pi_{\mathcal{D}} S^{\text{inj}}) k^+ + f(\pi_{\mathcal{D},\Delta t} S) k^-$. Then, one has

$$\begin{aligned} F_{\mathcal{D}}^n(\psi^{n-1}) &= \sum_{n=1}^N \int_{t_{n-1}}^{t_n} \int_{\Omega} \pi_{\mathcal{D},\Delta t} \psi(\mathbf{x}, t_{n-1}) k_{\mathcal{D},\Delta t}^o(\mathbf{x}, t) \, d\mathbf{x} dt \\ &\rightarrow \int_0^{t_f} \int_{\Omega} \bar{\psi}(\mathbf{x}, t) k^o(\mathbf{x}, \bar{S}(\mathbf{x}, t)) \, d\mathbf{x} dt \quad \text{as } h_{\mathcal{T}}, \Delta t \rightarrow 0. \end{aligned}$$

□

4 Numerical examples

We consider an homogeneous isotropic porous media of permeability $\Lambda = I$ and porosity $\phi = 1$ on the domain $\Omega = (0, 1)^d$, $d = 2, 3$. The domain is initially saturated with water $S_0 = 0$ and oil ($S = 1$) is injected at the left side $x = 0$ of the domain with a fixed total velocity $V_T = -\lambda(S)\Lambda \nabla P \cdot \mathbf{n} = 1$. On the right side $x = 1$, the oil saturation $S = 0$ and the global pressure $P = 1$ are imposed. Homogeneous Neumann boundary conditions are imposed on the remaining sides of the domain, and there is no source terms.

With such boundary conditions it is well known that the solution S, P of the two-phase flow model depends only on the x coordinate and on time t . The oil saturation $S(x, t)$ is the solution of the following one-dimensional Buckley Leverett degenerate parabolic equation

$$\left\{ \begin{array}{ll} \partial_t S + \partial_x f(S) - \partial_{x^2} \varphi(S) = 0 & \text{on } (0, 1) \times (0, t_f), \\ S = 1 & \text{on } \{x = 0\} \times (0, t_f), \\ S = 0 & \text{on } \{x = 1\} \times (0, t_f), \\ S|_{t=0} = 0 & \text{on } (0, 1), \end{array} \right. \quad (41)$$

and the pressure is obtained from the saturation by the following integral

$$P(x, t) = 1 + \int_x^1 \frac{du}{\lambda(S(u, t))}. \quad (42)$$

In our numerical experiment, the relative permeabilities are given by $k_{r,o}(S) = S^2$ and $k_{r,w}(S) = (1 - S)^2$ and the capillary pressure by $P_c(S) = -P_{c,1} \log(1 - S) + P_{c,0}$ where the parameter $P_{c,1} \geq 0$ will basically control the capillary diffusion of the saturation equation. The viscosity of the oil and water phases are chosen to be

$\mu_o = 5$ and $\mu_w = 1$ which leads to the following total mobility, fractional flow, and capillary diffusion functions

$$\lambda(S) = \frac{S^2}{5} + (1 - S)^2, \quad f(S) = \frac{\frac{S^2}{5}}{\frac{S^2}{5} + (1 - S)^2}, \quad \varphi(S) = \frac{P_{c,1}}{5} \int_0^S \frac{u^2(1 - u)}{\frac{u^2}{5} + (1 - u)^2} du.$$

Note that $\varphi(S)$ can be computed analytically.

The solution of the Buckley Leverett equation (41) and the pressure (42) are computed numerically on a uniform 1D mesh of size $n_x = 1000$ and with a time step $n_{subdt} = 20$ times smaller than the time step used for the solution on the VAG discretization on the domain $(0, 1)^d$.

Let S_e and P_e denote the discrete solutions of (41), (42) defined by a continuous cellwise linear interpolation in space and a constant interpolation in time on each of the $n_{subdt}N$ time sub-intervals. We define the following approximations of the $L^2(0, t_f, L^2(\Omega))$ norm of the errors for S, P :

$$\|eS\|^2 := \sum_{n=1}^N \Delta t \|\pi_{\mathcal{T}} S^n - S_e(t^n)\|_{L^2(\Omega)}^2,$$

$$\|eP\|^2 := \sum_{n=1}^N \Delta t \|\pi_{\mathcal{T}} P^n - P_e(t^n)\|_{L^2(\Omega)}^2.$$

For ∇P , we obtain the approximation of the $L^2(0, t_f, (L^2(\Omega))^d)$ error by

$$\|e\nabla P\|^2 := \sum_{n=1}^N \Delta t \|\nabla \pi_{\mathcal{T}} P^n - \nabla P_e(t^n)\|_{(L^2(\Omega))^d}^2.$$

The integrals in space are approximated using second order quadrature formulae in each triangle (in 2D) or tetrahedra (in 3D).

We also define the convergence rates for each of the above error norms $\|e\|$ between two successive meshes m and $m + 1$ in dimension d :

$$\tau_e = d \frac{\ln\left(\frac{\|e^m\|}{\|e^{m+1}\|}\right)}{\ln\left(\frac{\#\mathcal{V}_{int}^{m+1} \cup \mathcal{V}_N^{m+1}}{\#\mathcal{V}_{int}^m \cup \mathcal{V}_N^m}\right)}.$$

The numerical experiments are done using the FVCA5 benchmark triangular and Cartesian meshes in 2D and the FVCA6 benchmark tetrahedral, Cartesian, and prismatic meshes in 3D. We have also added quadrangular and hexahedral meshes obtained by random perturbation of the Cartesian meshes respectively for $d = 2, 3$.

Our main objective is to illustrate the convergence of the scheme independently of the choice of the volume given by the parameters α_{κ}^s . We will experiment three choices of these parameters. The first choice roughly balances the volumes at the vertices and at cells, the second choice sets very small volumes at the vertices, and the third choice is a random choice of the volumes at the vertices.

- Choice 1: $\alpha_{\kappa,s} = \omega \frac{1}{\#\mathcal{M}_s}$, for $\omega = 0.5$ in 2D and $\omega = 0.3$ in 3D.
- Choice 2: $\alpha_{\kappa,s} = \omega \frac{1}{\#\mathcal{M}_s}$, for $\omega = 0.01$.
- Choice 3: $\alpha_{\kappa,s} = \begin{cases} \omega \frac{1}{\#\mathcal{M}_s} & \text{if } \{\kappa \mid \text{rocktype}_\kappa = 2\} = \mathcal{M}_s, \\ \omega \frac{1}{\#\mathcal{M}_s} & \text{else if } \text{rocktype}_\kappa = 1, \\ 0 & \text{else if } \text{rocktype}_\kappa = 2. \end{cases}$

with $\omega = 0.5$ in 2D and 0.3 in 3D and for a random choice of the rocktype of the cells. This third choice mimics what is done in [17] to impose a single rocktype at the vertices for a porous media with two rocktypes.

We also investigate the influence of the capillary diffusion parameter $P_{c,1}$ on the convergence with three values of this parameter $P_{c,1} = 1$ or 0.1 or 0. Note that the value $P_{c,1} = 0$ is not covered by our theoretical analysis.

In all the above numerical experiments, the time step is constant, and the number of time steps is fixed to 1600 in dimension $d = 2$ and to 400 in dimension $d = 3$ in such a way that the time discretization error is kept small with respect to the space discretization error.

Figures 2 and 3 exhibit the convergence of the saturation on the 2D and 3D meshes for a small capillary diffusion $P_{c,1} = 0.1$ and the three choices of the volumes. It clearly shows the weak dependence of the solution on the choice of the parameters α_κ^s . In addition the accuracies obtained for the three different choices of the parameters α_κ^s are always in the same order: the best accuracy is obtained for the first choice, followed by the third choice and ending with the second choice. The same result holds for the global pressure and its gradient as can be checked in the tables below. It can easily be explained since, roughly speaking, the more balanced the volume between cells and vertices, the better the accuracy, which corresponds intuitively to an optimized refinement of the mesh.

Figures 4 and 5 compare the convergence of the saturation and of the global pressure on the different meshes for fixed choices of the capillary diffusion $P_{c,1} = 0.1$ and of the volumes. It exhibits that the convergence rate as a function of the number of nodes is roughly the same for the all these quasi uniform meshes as could be expected. Besides, the constant is quite close for all the 2D and 3D mesh families considered here.

Figures 6 and 7 compare the convergence of the saturation and of the global pressure for different choices of the capillary diffusion parameter $P_{c,1} = 1, 0.1, 0$, and fixed families of meshes (quadrangular meshes in 2D and hexahedral meshes in 3D) and a fixed choice of the volumes. This time, the convergence rate is clearly dependent on the capillary diffusion.

For $P_{c,1} = 0$, it is as expected lower than for $P_{c,1} = 0.1, 1$ due to the jump of the saturation at the chock. Although our convergence proof does not cover this case, the convergence is observed numerically whatever the choices of the volumes as can be seen in the tables 12 and 18 below.

For $P_{c,1} = 0.1$ or 1, the convergence rate for the saturation is expected to tend to 1 for a fine enough space discretization. This is clearly observed in 2D. In 3D it is not so clear for $P_{c,1} = 0.1$ certainly due to a too coarse space discretization compared with the 2D case.

5 Conclusion

The convergence of the VAG discretization of the two-phase Darcy flow model to a weak solution is shown whatever the choice of the volumes at the cell centers and at the vertices for general polyhedral meshes and permeability tensors. This is confirmed by the numerical experiments carried out for 2D and 3D families of meshes. They show that the solution is only slightly dependent on the choice of these volumes and exhibits a better accuracy when the volumes at the surrounding cells and vertices are more balanced. This is basically due to the fact that it amounts to a mesh refinement for the upwind approximation of the fractional flow term. We also notice in the numerical experiments that these results seem to extend to the case of no capillary diffusion not covered by our convergence analysis.

From these theoretical and numerical results, we deduce that the practical choice of the volumes at the cell centers and at the vertices can be done, as proposed in [17], in order first to respect the main heterogeneities of the porous media and second to balance as much as possible the volumes at the neighbouring cells and vertices.

Acknowledgements: We would like to thank the anonymous reviewers for their useful comments and remarks.

References

- [1] O. Angelini, K. Brenner, D. Hilhorst, A finite volume method on general meshes for a degenerate parabolic convection-reaction-diffusion equation, *Numer. Math.*, vol. 123, issue 2, pp. 219-257, 2013.
- [2] S. N. Antontsev, A. V. Kazhikhov, and V. N. Monakhov. *Boundary value problems in mechanics of nonhomogeneous fluids*, volume 22 of *Studies in Mathematics and its Applications*. North-Holland Publishing Co., Amsterdam, 1990. Translated from the Russian.
- [3] K. Aziz and A. Settari, *Petroleum Reservoir Simulation*, Applied Science Publishers, 1979.
- [4] B.R. Baliga and S.V. Patankar SV, A control volume finite-element method for two dimensional fluid flow and heat transfer. *Numerical Heat Transfer*, vol. 6, pp. 245-261, 1983.
- [5] K. Brenner, *Méthodes Volume Finis sur maillage quelconques pour des systèmes d'évolution non linéaires*. Thèse de Doctorat, 2011.

- [6] G. Chavent and J. Jaffr. *Mathematical Models and Finite Elements for Reservoir Simulation*, volume 17. North-Holland, Amsterdam, stud. math. appl. edition, 1986.
- [7] Z. Chen, On the control volume finite element methods and their applications to multiphase flow, *Networks and Heterogeneous Media*, American Institute of Mathematical Sciences, vol. 1,4, December, 2006.
- [8] Z. Chen and R. E. Ewing. Degenerate two-phase incompressible flow. III. Sharp error estimates. *Numer. Math.*, 90(2) pp. 215-240, 2001.
- [9] Z. Chen. Degenerate two-phase incompressible flow. I. Existence, uniqueness and regularity of a weak solution. *J. Differential Equations*, 171(2) pp. 203-232, 2001.
- [10] A. Ern and J.L. Guermond, *Theory and Practice of Finite Elements*, vol. 159 of Applied Mathematical Series, Springer, New York, 2004.
- [11] R. Eymard, P. Féron, T. Gallouët, R. Herbin, C. Guichard. Gradient schemes for the Stefan problem. *IJFV - International Journal on Finite Volumes*, 2013.
- [12] R. Eymard, R. Herbin, and A. Michel. Mathematical study of a petroleum-engineering scheme. *M2AN Math. Model. Numer. Anal.*, 37(6) pp. 937-972, 2003.
- [13] R. Eymard, and T. Gallouët, and R. Herbin, Discretisation of heterogeneous and anisotropic diffusion problems on general non-conforming meshes, *SUSHI: a scheme using stabilisation and hybrid interfaces*. *IMA Journal on Numerical Analysis*, 30,4, pp. 1009-1043, 2010.
- [14] R. Eymard, C. Guichard, and R. Herbin, Benchmark 3D: the VAG scheme. In *Finite Volumes for Complex Applications VI – Problems and Perspectives*. Fort, J. and Furst, J. and Halama, J. and Herbin, R. and Hubert, F. editors, Springer Proceedings in Mathematics, 2, pp. 213-222, 2011.
- [15] R. Eymard, G. Henry, R. Herbin, F. Hubert, R. Klöfkorn, and G. Manzini, Benchmark 3d on discretization schemes for anisotropic diffusion problem on general grids. In *Finite Volumes for Complex Applications VI – Problems and Perspectives*. Fort, J. and Furst, J. and Halama, J. and Herbin, R. and Hubert, F. editors, Springer Proceedings in Mathematics, 2, pp. 95–265, 2011.
- [16] R. Eymard, C. Guichard, and R. Herbin, Small-stencil 3D schemes for diffusive flows in porous media. *ESAIM: Mathematical Modelling and Numerical Analysis*, 46, pp. 265-290, 2010.
- [17] R. Eymard, R. Herbin, C. Guichard, R. Masson, Vertex Centered discretization of compositional Multiphase Darcy flows on general meshes. *Comp. Geosciences*, vol. 16, issue 4, pp. 987-1005, 2012.
- [18] R. Eymard, R. Herbin, C. Guichard, R. Masson, Vertex Centered discretization of Two-Phase Darcy flows on general meshes. *ESAIM Proc.* vol. 35, pp. 59-78, 2012.

- [19] R. Huber and R. Helmig, Node-centered finite volume discretizations for the numerical simulation of multi-phase flow in heterogeneous porous media, *Computational Geosciences*, 4, pp. 141-164, 2000.
- [20] A. Michel, A finite volume scheme for two-phase immiscible flow in porous media, *SIAM J. Numer. Anal.*, 41(4), pp. 1301–1317, 2003.
- [21] D. W. Peaceman, *Fundamentals of Numerical Reservoir Simulations*, Elsevier, 1977.

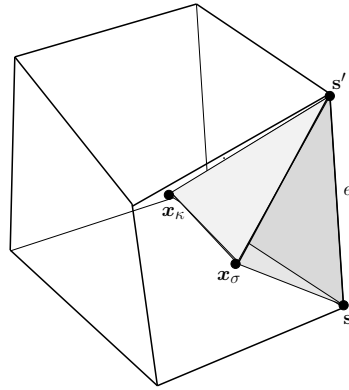


Figure 1: Tetrahedron $T_{\kappa,\sigma,e}$ of the sub-mesh \mathcal{T} .

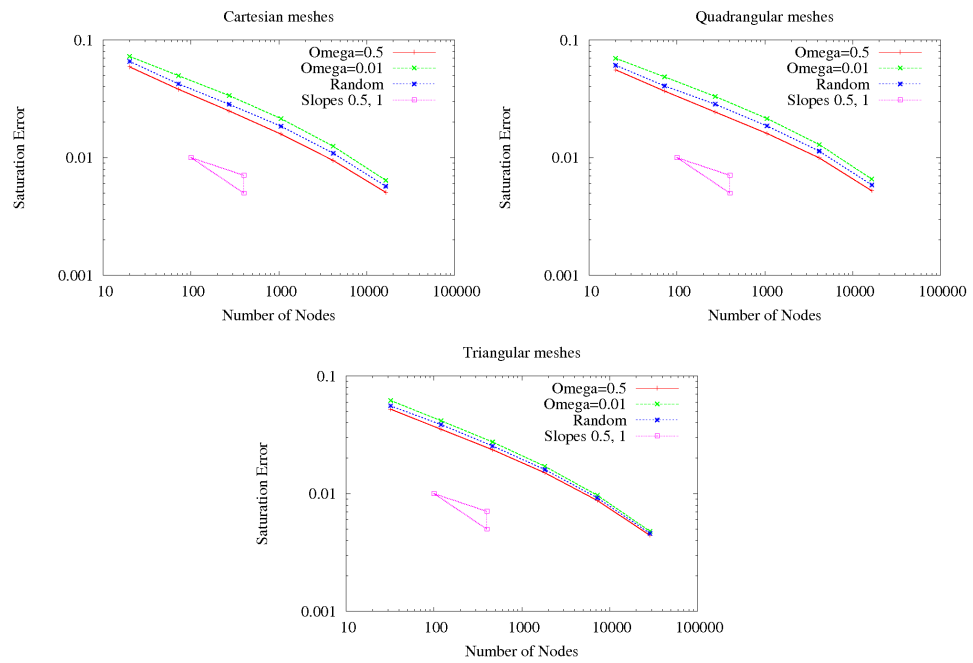


Figure 2: $L^2(0, t_f, L^2(\Omega))$ errors for the saturation S on the Cartesian, quadrangular and triangular meshes, $P_{c,1} = 0.1$.

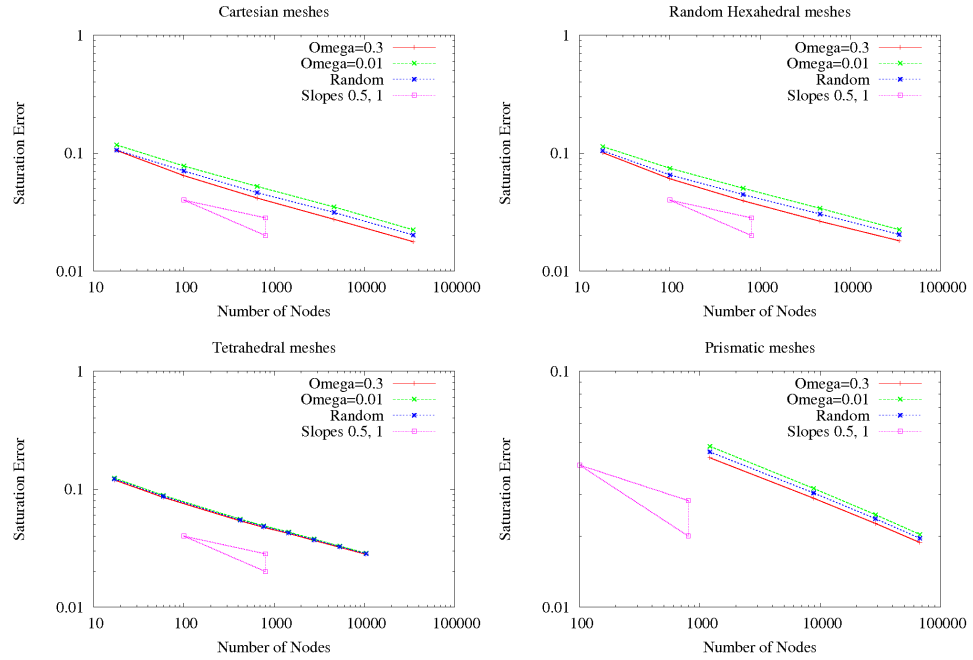


Figure 3: $L^2(0, t_f, L^2(\Omega))$ errors for the saturation S on the Cartesian, hexahedral, tetrahedral and prismatic meshes, $P_{c,1} = 0.1$.

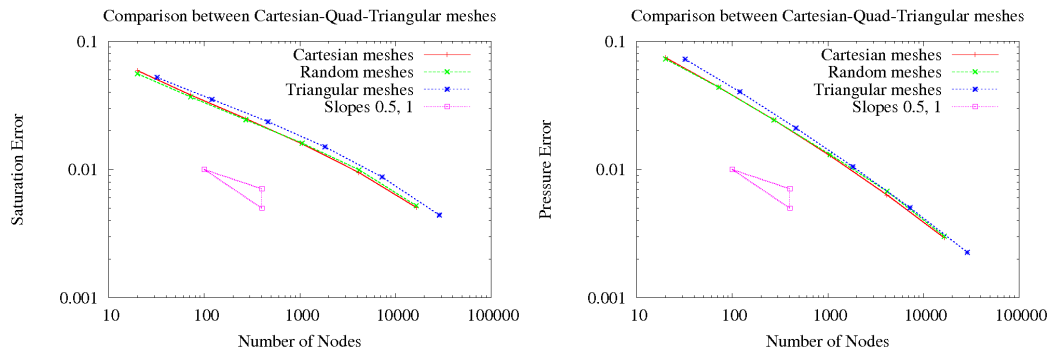


Figure 4: $L^2(0, t_f, L^2(\Omega))$ errors for S, P on the cartesian, quadrangular, and triangular meshes with choice 1 of α_{κ}^s and $P_{c,1} = 0.1$.

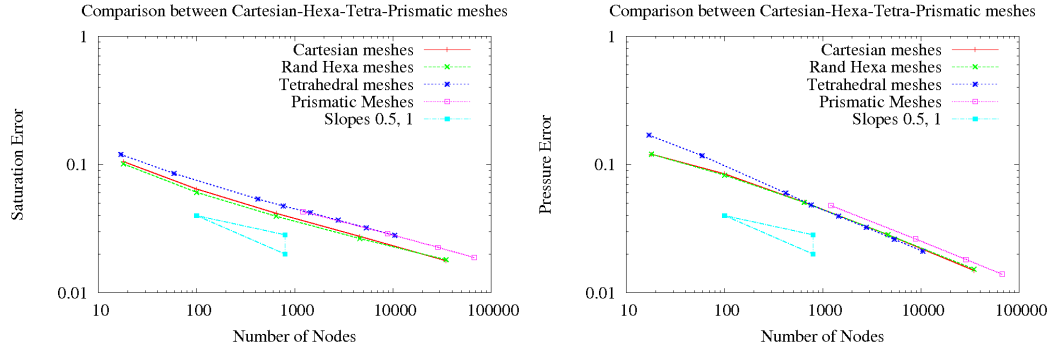


Figure 5: $L^2(0, t_f, L^2(\Omega))$ errors for S, P on the cartesian, hexahedral, tetrahedral, and prismatic meshes with choice 1 of α_κ^S and $P_{c,1} = 0.1$.

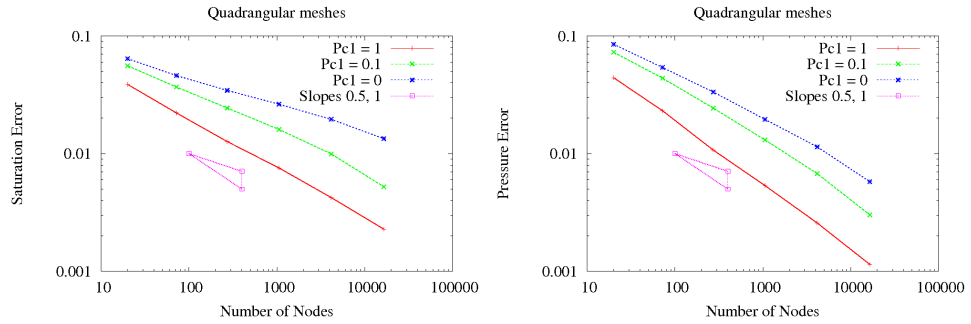


Figure 6: $L^2(0, t_f, L^2(\Omega))$ errors for S, P on the quadrangular meshes, the first choice of α_κ^S , and the capillary diffusion parameter $P_{c,1} = 1, 0.1, 0$.

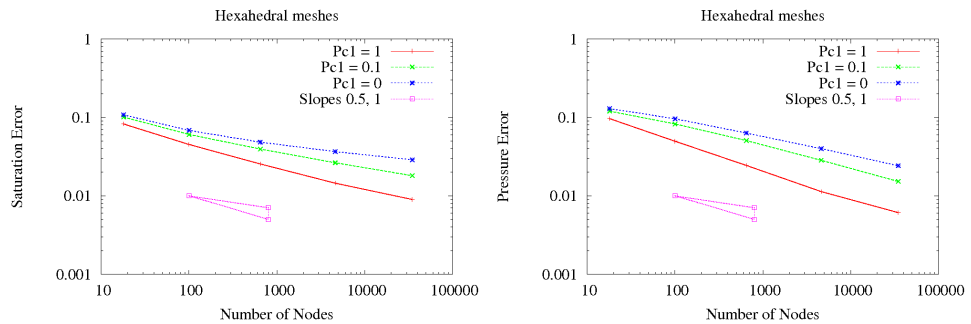


Figure 7: $L^2(0, t_f, L^2(\Omega))$ errors for S, P on the hexahedral meshes, the first choice of α_κ^S , and the capillary diffusion parameter $P_{c,1} = 1, 0.1, 0$.

$\#(\mathcal{V}_{int} \cup \mathcal{V}_N)$	$\ e_S\ $	τ_{e_S}	$\ e_P\ $	τ_{e_P}	$\ e_{\nabla P}\ $	$\tau_{e_{\nabla P}}$
20	0.59E-01		0.75E-01		0.34	
72	0.38E-01	0.69	0.44E-01	0.83	0.23	0.62
272	0.25E-01	0.64	0.24E-01	0.88	0.15	0.61
1056	0.16E-01	0.67	0.13E-01	0.95	0.10	0.64
4160	0.95E-02	0.75	0.63E-02	1.02	0.62E-01	0.69
16512	0.51E-02	0.91	0.29E-02	1.12	0.36E-01	0.80
20	0.72E-01		0.13		0.45	
72	0.50E-01	0.59	0.74E-01	0.87	0.30	0.65
272	0.34E-01	0.59	0.39E-01	0.97	0.19	0.67
1056	0.21E-01	0.66	0.19E-01	1.08	0.12	0.69
4160	0.12E-01	0.79	0.84E-02	1.18	0.72E-01	0.72
16512	0.64E-02	0.97	0.35E-02	1.26	0.41E-01	0.83
20	0.66E-01		0.96E-01		0.43	
72	0.42E-01	0.69	0.55E-01	0.88	0.25	0.83
272	0.28E-01	0.60	0.30E-01	0.92	0.17	0.62
1056	0.19E-01	0.63	0.15E-01	0.97	0.11	0.64
4160	0.11E-01	0.77	0.72E-02	1.10	0.67E-01	0.70
16512	0.57E-02	0.94	0.32E-02	1.19	0.38E-01	0.81

Figure 8: Convergence of the L^2 error for S , P and ∇P for the 2D Cartesian meshes with $P_{c,1} = 0.1$ and the three choices 1, 2, 3 in this order of α_k^s .

$\#(\mathcal{V}_{int} \cup \mathcal{V}_N)$	$\ e_S\ $	τ_{eS}	$\ e_P\ $	τ_{eP}	$\ e_{\nabla P}\ $	$\tau_{e_{\nabla P}}$
20	0.56E-01		0.73E-01		0.33	
72	0.37E-01	0.65	0.44E-01	0.79	0.23	0.60
272	0.24E-01	0.62	0.24E-01	0.88	0.15	0.61
1056	0.16E-01	0.62	0.13E-01	0.92	0.10	0.59
4160	0.10E-01	0.70	0.68E-02	0.96	0.66E-01	0.63
16512	0.52E-02	0.93	0.30E-02	1.17	0.37E-01	0.84
20	0.70E-01		0.13		0.43	
72	0.49E-01	0.57	0.74E-01	0.85	0.29	0.63
272	0.33E-01	0.58	0.39E-01	0.95	0.19	0.67
1056	0.21E-01	0.64	0.19E-01	1.08	0.12	0.66
4160	0.13E-01	0.74	0.89E-02	1.10	0.75E-01	0.67
16512	0.66E-02	0.98	0.36E-02	1.30	0.41E-01	0.87
20	0.61E-01		0.92E-01		0.36	
72	0.41E-01	0.63	0.53E-01	0.87	0.25	0.60
272	0.28E-01	0.54	0.30E-01	0.84	0.17	0.60
1056	0.19E-01	0.63	0.16E-01	0.97	0.11	0.63
4160	0.11E-01	0.72	0.77E-02	1.03	0.70E-01	0.64
16512	0.59E-02	0.96	0.33E-02	1.23	0.39E-01	0.85

Figure 9: Convergence of the L^2 error for S , P and ∇P for the 2D quadrangular meshes with $P_{c,1} = 0.1$ and the three choices 1, 2, 3 in this order of α_k^s .

$\#(\mathcal{V}_{int} \cup \mathcal{V}_N)$	$\ e_S\ $	τ_{e_S}	$\ e_P\ $	τ_{e_P}	$\ e_{\nabla P}\ $	$\tau_{e_{\nabla P}}$
32	0.52E-01		0.72E-01		0.32	
120	0.35E-01	0.59	0.40E-01	0.89	0.20	0.68
464	0.24E-01	0.59	0.21E-01	0.96	0.13	0.64
1824	0.15E-01	0.66	0.11E-01	1.01	0.87E-01	0.60
7232	0.87E-02	0.79	0.50E-02	1.07	0.55E-01	0.66
28800	0.44E-02	0.99	0.23E-02	1.16	0.30E-01	0.87
32	0.62E-01		0.96E-01		0.36	
120	0.42E-01	0.60	0.51E-01	0.97	0.22	0.70
464	0.27E-01	0.62	0.25E-01	1.05	0.14	0.67
1824	0.17E-01	0.70	0.12E-01	1.10	0.93E-01	0.62
7232	0.97E-02	0.82	0.54E-02	1.14	0.59E-01	0.68
28800	0.48E-02	1.02	0.23E-02	1.20	0.32E-01	0.88
32	0.56E-01		0.80E-01		0.34	
120	0.39E-01	0.55	0.45E-01	0.87	0.21	0.69
464	0.25E-01	0.62	0.23E-01	1.00	0.14	0.66
1824	0.16E-01	0.67	0.11E-01	1.06	0.90E-01	0.61
7232	0.92E-02	0.81	0.52E-02	1.10	0.57E-01	0.67
28800	0.46E-02	1.01	0.23E-02	1.18	0.31E-01	0.88

Figure 10: Convergence of the L^2 error for S , P and ∇P for the 2D triangular meshes with $P_{c,1} = 0.1$ and the three choices 1, 2, 3 in this order of α_k^s .

$\#(\mathcal{V}_{int} \cup \mathcal{V}_N)$	$\ e_S\ $	τ_{e_S}	$\ e_P\ $	τ_{e_P}	$\ e_{\nabla P}\ $	$\tau_{e_{\nabla P}}$
20	0.39E-01		0.44E-01		0.27	
72	0.22E-01	0.87	0.23E-01	1.01	0.16	0.78
272	0.13E-01	0.84	0.11E-01	1.16	0.92E-01	0.86
1056	0.76E-02	0.76	0.54E-02	1.02	0.54E-01	0.79
4160	0.42E-02	0.84	0.26E-02	1.07	0.29E-01	0.89
16512	0.23E-02	0.90	0.11E-02	1.18	0.14E-01	1.03
20	0.47E-01		0.77E-01		0.31	
72	0.27E-01	0.85	0.34E-01	1.30	0.18	0.89
272	0.15E-01	0.90	0.14E-01	1.36	0.97E-01	0.90
1056	0.84E-02	0.86	0.59E-02	1.23	0.56E-01	0.82
4160	0.45E-02	0.91	0.28E-02	1.12	0.30E-01	0.90
16512	0.24E-02	0.94	0.12E-02	1.21	0.15E-01	1.04
20	0.42E-01		0.57E-01		0.28	
72	0.24E-01	0.85	0.26E-01	1.20	0.17	0.80
272	0.14E-01	0.85	0.12E-01	1.23	0.95E-01	0.87
1056	0.79E-02	0.82	0.56E-02	1.07	0.55E-01	0.82
4160	0.44E-02	0.87	0.26E-02	1.10	0.30E-01	0.89
16512	0.23E-02	0.91	0.12E-02	1.19	0.15E-01	1.04

Figure 11: Convergence of the L^2 error for S , P and ∇P for the 2D quadrangular meshes with $P_{c,1} = 1$ and the three choices 1, 2, 3 in this order of α_κ^s .

$\#(\mathcal{V}_{int} \cup \mathcal{V}_N)$	$\ eS\ $	τ_{eS}	$\ eP\ $	τ_{eP}	$\ e\nabla P\ $	$\tau_{e\nabla P}$
20	0.64E-01		0.85E-01		0.35	
72	0.46E-01	0.52	0.54E-01	0.71	0.25	0.56
272	0.34E-01	0.44	0.33E-01	0.72	0.17	0.56
1056	0.26E-01	0.40	0.20E-01	0.79	0.12	0.55
4160	0.20E-01	0.43	0.11E-01	0.78	0.81E-01	0.54
16512	0.13E-01	0.55	0.58E-02	0.99	0.54E-01	0.57
20	0.79E-01		0.14		0.48	
72	0.59E-01	0.45	0.91E-01	0.71	0.34	0.54
272	0.46E-01	0.39	0.56E-01	0.73	0.24	0.55
1056	0.36E-01	0.36	0.34E-01	0.75	0.16	0.54
4160	0.28E-01	0.37	0.20E-01	0.73	0.11	0.53
16512	0.20E-01	0.45	0.11E-01	0.88	0.77E-01	0.57
20	0.69E-01		0.11		0.40	
72	0.51E-01	0.50	0.65E-01	0.78	0.28	0.54
272	0.40E-01	0.36	0.43E-01	0.63	0.20	0.50
1056	0.31E-01	0.37	0.26E-01	0.74	0.14	0.56
4160	0.24E-01	0.38	0.16E-01	0.73	0.95E-01	0.52
16512	0.17E-01	0.48	0.83E-02	0.91	0.65E-01	0.57

Figure 12: Convergence of the L^2 error for S , P and ∇P for the 2D quadrangular meshes with $P_{c,1} = 0$ (no capillary diffusion) and the three choices 1, 2, 3 in this order of α_κ^s .

$\#(\mathcal{V}_{int} \cup \mathcal{V}_N)$	$\ eS\ $	τ_{eS}	$\ eP\ $	τ_{eP}	$\ e\nabla P\ $	$\tau_{e\nabla P}$
18	0.11		0.12		0.52	
100	0.64E-01	0.86	0.85E-01	0.62	0.39	0.51
648	0.42E-01	0.70	0.51E-01	0.82	0.26	0.65
4624	0.27E-01	0.63	0.28E-01	0.89	0.17	0.66
34848	0.18E-01	0.65	0.15E-01	0.96	0.11	0.66
18	0.12		0.20		0.66	
100	0.78E-01	0.72	0.13	0.79	0.47	0.61
648	0.52E-01	0.64	0.75E-01	0.89	0.31	0.68
4624	0.35E-01	0.61	0.40E-01	0.96	0.19	0.69
34848	0.22E-01	0.66	0.20E-01	1.05	0.12	0.68
18	0.11		0.15		0.58	
100	0.71E-01	0.72	0.10	0.69	0.42	0.54
648	0.46E-01	0.68	0.60E-01	0.83	0.28	0.68
4624	0.31E-01	0.59	0.34E-01	0.87	0.18	0.65
34848	0.20E-01	0.65	0.17E-01	0.99	0.11	0.67

Figure 13: Convergence of the L^2 error for S , P and ∇P for the 3D Cartesian meshes with $P_{c,1} = 0.1$ and the three choices 1, 2, 3 in this order of α_κ^s .

$\#(\mathcal{V}_{int} \cup \mathcal{V}_N)$	$\ eS\ $	τ_{eS}	$\ eP\ $	τ_{eP}	$\ e\nabla P\ $	$\tau_{e\nabla P}$
18	0.10		0.12		0.50	
100	0.61E-01	0.89	0.83E-01	0.66	0.37	0.54
648	0.40E-01	0.69	0.51E-01	0.78	0.25	0.63
4624	0.26E-01	0.61	0.28E-01	0.89	0.16	0.65
34848	0.18E-01	0.56	0.15E-01	0.92	0.11	0.59
18	0.11		0.20		0.65	
100	0.75E-01	0.74	0.13	0.81	0.45	0.65
648	0.50E-01	0.63	0.74E-01	0.87	0.30	0.66
4624	0.34E-01	0.60	0.40E-01	0.95	0.19	0.68
34848	0.22E-01	0.62	0.20E-01	1.04	0.12	0.64
18	0.10		0.14		0.54	
100	0.65E-01	0.82	0.94E-01	0.66	0.39	0.54
648	0.45E-01	0.62	0.60E-01	0.73	0.27	0.60
4624	0.30E-01	0.58	0.34E-01	0.86	0.18	0.66
34848	0.20E-01	0.59	0.18E-01	0.98	0.12	0.61

Figure 14: Convergence of the L^2 error for S , P and ∇P for the 3D Hexahedral meshes with $P_{c,1} = 0.1$ and the three choices 1, 2, 3 in this order of α_κ^s .

$\#(\mathcal{V}_{int} \cup \mathcal{V}_N)$	$\ eS\ $	τ_{eS}	$\ eP\ $	τ_{eP}	$\ e\nabla P\ $	$\tau_{e\nabla P}$
766	0.47E-01	0.63	0.48E-01	1.08	0.24	0.74
1452	0.42E-01	0.56	0.40E-01	0.93	0.21	0.64
2777	0.37E-01	0.63	0.32E-01	0.94	0.18	0.63
5356	0.32E-01	0.62	0.26E-01	0.97	0.16	0.59
10468	0.28E-01	0.61	0.21E-01	0.98	0.14	0.56
766	0.49E-01	0.65	0.51E-01	1.12	0.24	0.75
1452	0.43E-01	0.58	0.41E-01	0.97	0.21	0.65
2777	0.38E-01	0.64	0.33E-01	0.96	0.18	0.64
5356	0.33E-01	0.63	0.27E-01	1.00	0.16	0.60
10468	0.29E-01	0.62	0.21E-01	1.00	0.14	0.56
766	0.48E-01	0.64	0.49E-01	1.11	0.24	0.74
1452	0.43E-01	0.57	0.40E-01	0.95	0.21	0.65
2777	0.37E-01	0.63	0.33E-01	0.94	0.18	0.63
5356	0.33E-01	0.62	0.26E-01	0.99	0.16	0.59
10468	0.28E-01	0.61	0.21E-01	0.99	0.14	0.56

Figure 15: Convergence of the L^2 error for S , P and ∇P for the 3D tetrahedral meshes with $P_{c,1} = 0.1$ and the three choices 1, 2, 3 in this order of α_κ^s .

$\#(\mathcal{V}_{int} \cup \mathcal{V}_N)$	$\ eS\ $	τ_{eS}	$\ eP\ $	τ_{eP}	$\ e\nabla P\ $	$\tau_{e\nabla P}$
1210	0.43E-01		0.48E-01		0.25	
8820	0.29E-01	0.60	0.26E-01	0.91	0.16	0.66
28830	0.23E-01	0.62	0.18E-01	0.93	0.13	0.61
67240	0.19E-01	0.66	0.14E-01	0.94	0.11	0.59
1210	0.48E-01		0.57E-01		0.26	
8820	0.32E-01	0.62	0.30E-01	0.98	0.17	0.68
28830	0.25E-01	0.65	0.20E-01	1.00	0.13	0.63
67240	0.20E-01	0.68	0.15E-01	1.00	0.11	0.60
1210	0.45E-01		0.52E-01		0.25	
8820	0.30E-01	0.60	0.28E-01	0.94	0.16	0.67
28830	0.24E-01	0.64	0.19E-01	0.97	0.13	0.62
67240	0.20E-01	0.67	0.15E-01	0.97	0.11	0.60

Figure 16: Convergence of the L^2 error for S , P and ∇P for the 3D prismatic meshes with $P_{c,1} = 0.1$ and the three choices 1, 2, 3 in this order of α_κ^s .

$\#(\mathcal{V}_{int} \cup \mathcal{V}_N)$	$\ eS\ $	τ_{eS}	$\ eP\ $	τ_{eP}	$\ e\nabla P\ $	$\tau_{e\nabla P}$
18	0.82E-01		0.97E-01		0.46	
100	0.45E-01	1.05	0.50E-01	1.16	0.30	0.77
648	0.26E-01	0.92	0.24E-01	1.14	0.18	0.85
4624	0.14E-01	0.87	0.11E-01	1.17	0.99E-01	0.89
34848	0.90E-02	0.70	0.61E-02	0.92	0.60E-01	0.72
18	0.91E-01		0.15		0.55	
100	0.53E-01	0.95	0.78E-01	1.13	0.33	0.87
648	0.30E-01	0.92	0.34E-01	1.30	0.19	0.92
4624	0.16E-01	0.93	0.14E-01	1.32	0.10	0.92
34848	0.96E-02	0.80	0.68E-02	1.11	0.62E-01	0.77
18	0.85E-01		0.11		0.48	
100	0.48E-01	1.01	0.58E-01	1.03	0.31	0.78
648	0.28E-01	0.89	0.28E-01	1.16	0.18	0.84
4624	0.15E-01	0.89	0.13E-01	1.20	0.10	0.90
34848	0.93E-02	0.75	0.65E-02	1.02	0.61E-01	0.75

Figure 17: Convergence of the L^2 error for S , P and ∇P for the 3D Hexahedral meshes with $P_{c,1} = 1$ and the three choices 1, 2, 3 in this order of α_κ^s .

$\#(\mathcal{V}_{int} \cup \mathcal{V}_N)$	$\ e_S\ $	τ_{eS}	$\ e_P\ $	τ_{eP}	$\ e_{\nabla P}\ $	$\tau_{e\nabla P}$
18	0.11		0.13		0.52	
100	0.68E-01	0.80	0.96E-01	0.52	0.40	0.46
648	0.48E-01	0.55	0.63E-01	0.68	0.28	0.56
4624	0.37E-01	0.43	0.40E-01	0.70	0.20	0.56
34848	0.29E-01	0.36	0.24E-01	0.75	0.14	0.54
18	0.12		0.22		0.68	
100	0.83E-01	0.67	0.14	0.72	0.49	0.57
648	0.60E-01	0.50	0.92E-01	0.72	0.35	0.57
4624	0.46E-01	0.41	0.57E-01	0.73	0.24	0.56
34848	0.36E-01	0.36	0.35E-01	0.75	0.17	0.54
18	0.11		0.15		0.56	
100	0.73E-01	0.74	0.11	0.55	0.43	0.46
648	0.54E-01	0.49	0.74E-01	0.61	0.31	0.51
4624	0.42E-01	0.39	0.48E-01	0.66	0.22	0.55
34848	0.33E-01	0.35	0.30E-01	0.72	0.15	0.53

Figure 18: Convergence of the L^2 error for S , P and ∇P for the 3D Hexahedral meshes with $P_{c,1} = 0$ and the three choices 1, 2, 3 in this order of α_κ^S .